WSG-Type Modular Expansion Joints

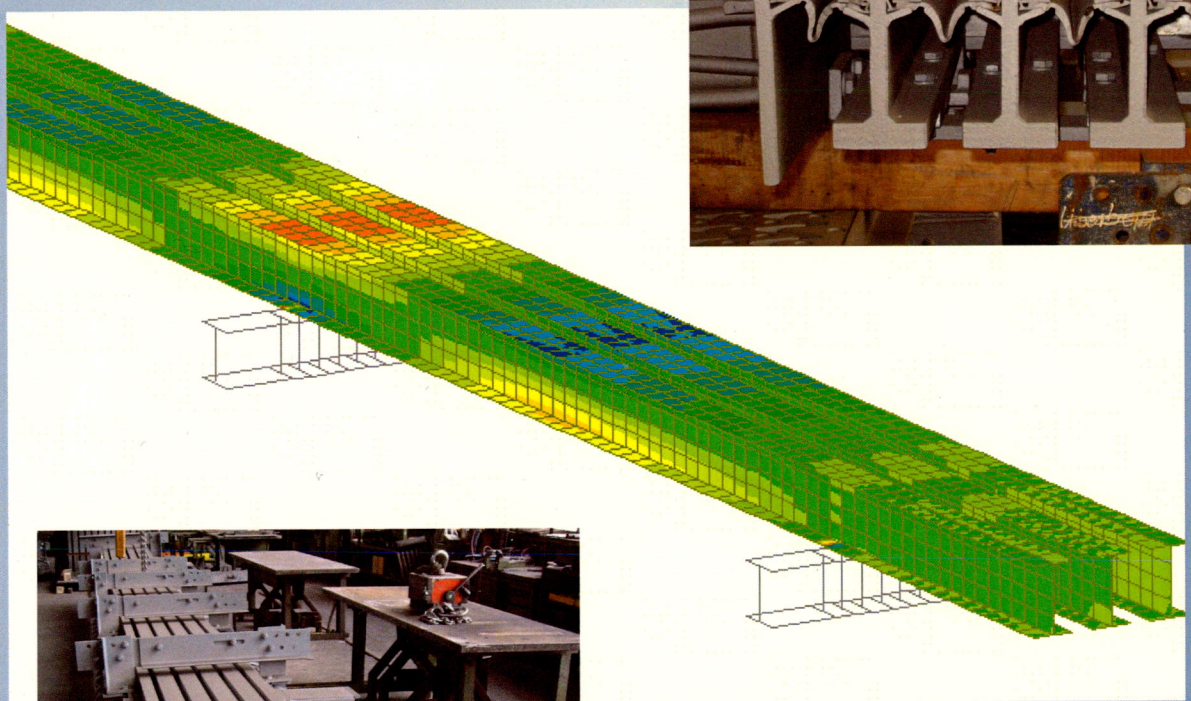

A study into the structural behaviour of modular expansion joints of Sollinger Hütte

H. Koop

WSG-Type Modular Expansion Joints

A study into the structural behaviour of modular expansion joints of Sollinger Hütte

Report

Master of Science Thesis
October 2007

Author: H. Koop

Delft University of Technology
Faculty of Civil Engineering and Geosciences
Department of Design and Construction
Delft, the Netherlands

Ministry of Transport, Public Works and Water Management
Bouwdienst Rijkswaterstaat
Department SWI
Utrecht, the Netherlands

RW Sollinger Hütte GmbH
Uslar, Germany

Master of Science Thesis
October 2007

Student:

Hendri Koop
Contact: hendri.koop@gmail.com

Graduation Committee:

Prof. ir. F.S.K. Bijlaard (chairman)	– Delft University of Technology, Faculty of Civil Engineering
Dr. ing. A. Romeijn	– Delft University of Technology, Faculty of Civil Engineering
Dr. ir. P.C.J. Hoogenboom	– Delft University of Technology, Faculty of Civil Engineering
Ing. J.S. Leendertz	– Bouwdienst Rijkswaterstaat
Dipl.-Ing. T. Schulze	– RW Sollinger Hütte GmbH
Ir. L.J.M. Houben (graduation coordinator)	– Delft University of Technology, Faculty of Civil Engineering

Preface

This report is the final result of a study performed at the Faculty of Civil Engineering and Geosciences of Delft University of Technology in order to obtain the Master of Science-degree in Civil Engineering. Subject of research are the modular expansion joints produced by the German company RW Sollinger Hütte GmbH.

Readers, who are interested in how the Sollinger Hütte WSG-type modular expansion joints are composed and function, should read paragraph 3.1. Those interested in the results of the numerical analysis made with the finite element program MIDAS/Civil and which parameters are important for the structural behaviour, should read chapter 8.

My gratitude goes to ing. Leendertz for his guidance during the thesis and arranging a work place at the Bouwdienst of Rijkswaterstaat in Utrecht. Also I would like to thank prof. Bijlaard, dr. Romeijn and dr. Hoogenboom for their contribution as members of my graduation committee.
Special thanks goes to dipl.-ing. Schulze of RW Sollinger Hütte GmbH for providing the necessary information and making it possible for me to visit the company in Uslar, Germany.

Delft, October 2007

Hendri Koop

Abstract

Expansion joints are applied in bridge structures to provide a smooth transition between the abutment and the superstructure of the bridge for traffic and to enable movements of the bridge structure. For long span bridge structures mainly joints belonging to the family of modular expansion joints are used in the Netherlands.
The basic concept of modular expansion joints is over 30 years old and consists of centre beams placed in transverse direction of the bridge supported by beams in traffic direction. Nowadays there are several manufacturers with their own variations in design to the basic concept. For historical reasons, many bridges in the Netherlands are equipped with joints made by the German company Maurer Söhne GmbH & Co. KG. Recent graduation works at TU Delft elaborated on joints produced by this company. Another German company that produces modular expansion joints is RW Sollinger Hütte GmbH. Their type is produced under the name "WSG Lamellen-Dehnfuge" and has been applied in Bridge Heteren, which is subject of a case study during this research.

Current design and construction is based on many years of experience and simple two-dimensional line models, and the dynamic behaviour is often determined with over-rolling test. The joints however have a strong three-dimensional behaviour.
This research has been performed in order to obtain a better understanding of the structural behaviour of WSG-type modular expansion joints made by Sollinger Hütte. Therefore, analytical calculations and a numerical analysis were performed. The analytical calculations have been made according to Annex G of the "Guideline for European Technical Approval of Expansion Joints for Road Bridges", which is composed by the "European Organisation for Technical Approvals", as it was at the end of 2006. For the numerical analysis a finite element model of the WSG 320-joint was constructed. The manufacturer has provided the necessary information about the WSG-type joints of Bridge Heteren and the finite element model was made with the use of the analysis program MIDAS/Civil.

For this analytical analysis a simple two-dimensional model has been used in which the traffic load was placed at the most unfavourable position without taking the distribution of traffic lanes into account. Verification of the static strength has shown that the centre beams, support bars and support bar bearings have sufficient capacity to withstand the traffic loads. The values for the unity checks already gave reason to expect that the support bar would be the governing structural element for the fatigue life of the expansion joint. The field of one of the support bars was therefore one of four cross-sections of the structure for which the fatigue damage and the fatigue lifetime has been determined as part of the fatigue assessment with Fatigue load Model 2 ($FLM2_{EJ}$) of Annex G, equivalent to EN 1991-2 FLM 4. The results indicate a more unfavourable behaviour than the original design calculations that showed no fatigue damage within the design lifetime of 30 years. By studying the influence of the partial fatigue strength factor it has been shown that regular inspection and maintenance are very beneficial with respect to ensuring a long lifetime.

While establishing the finite element model of the WSG 320-joint for the numerical analysis some aspects were recognized that are relevant to consider during the pre-processing phase. First of all modelling the axle loads needs to be done very accurate, but depends on the detail level at which the structure is modelled. Refining the mesh of those elements that form the contact surface allows a better description of the load functions. Furthermore it is noted that for the moment modelling of the friction between sliding plates is difficult to achieve with the analysis software used.

The numerical analyses for the reference model and the modified reference model, produced results that lead to a clear view on the structural behaviour of the WSG-type expansion joint.
The most relevant results are as follows:

- The frequency analysis showed that although low values are found for the first natural frequencies compared to those found in literature, the modes that govern the system behaviour have higher frequencies (> 132,8 Hz for the vertical motion);
- Dynamic properties of the control spring and the length of spans for centre beams are important for the dynamic and fatigue behaviour;

- Table 1 and 2 shows dynamic amplification factors found. The reference model leads to higher values than those included in the fatigue loads of Annex G. The modified reference model gives factors that are more favourable for the vertical and worse for the horizontal loading;
- When a situation with vertical and horizontal loading is considered, a phase shift can occur between the time points of maximum amplification for each load directions. If this happens the governing phase combination must be applied in the fatigue analysis of a centre beam;
- Comparison of a fatigue analysis for both models shows that the modifications taken into account in the modified reference model have a positive influence on the fatigue behaviour.

Table 1 Dynamic factors for the reference model.

	Centre beam			Support bar	
Wheel print	300 x 300	400 x 400		300 x 300	400 x 400
Force direction	Vertical	Vertical	Horizontal	Vertical	Vertical
First dynamic amplitude	2.1	1.9	3.0	1.6	2.1
Upswing ratio	1.2	1.1	1.2	1.2	1.0
Dynamic interval	2.5	2.1	3.7	1.8	2.2

Table 2 Dynamic factors for the modified reference model.

	Centre beam			Support bar	
Wheel print	300 x 300	400 x 400		300 x 300	400 x 400
Force direction	Vertical	Vertical	Horizontal	Vertical	Vertical
First dynamic amplitude	0.7	0.8	1.1	1.1	1.4
Upswing ratio	1.0	1.1	1.3	1.2	1.2
Dynamic interval	0.7	0.8	1.4	1.3	1.7

The research has lead to recommendations concerning modular expansion joints and fatigue. In short the recommendations that are considered most important are:

- Investigate the structural behaviour of larger WSG-type modular expansion joints of Sollinger-Hütte that can cope with much larger translations than the WSG 320-joint, as these joints almost completely rely on friction between components;
- Study the modular expansion joints of a different company. Subject could be the Tensa modular type LR made by Mageba or the Swivel joist expansion joint by Maurer Söhne;
- It is recommended to study the dynamic characteristics of the control springs in order to obtain more accurate values for the different stiffnesses.
- It is recommended to study the effects of the actual traffic data in comparison to the traffic data as presented in the standards. If this is done there will be a more realistic expectation about the fatigue life of the expansion joints;

For future calculations on the WSG-joints of Bridge Heteren the modelling presented in this study can be applied. However, it is advised to keep in mind that the axle load has been placed at the most adverse position without considering the distribution of the traffic lanes.

Table of contents

1. Introduction

Expansion joints are small structural components compared to the size of the bridges in which they can be found. Nevertheless these joints are important in the overall performance of a bridge. However, expansion joints are fragile and require frequent inspection and maintenance. Premature loss of function of an expansion joint does not only pose a treat to traffic safety, but can lead to more damage of the joint itself and damage of the bridge structure.
In the Netherlands Rijkswaterstaat, as a part of the Ministry of Transport, Public Works and Water Management, is responsible for the operation and maintenance of all public works. This includes the expansion joints in bridge structures for road traffic. Annually the Bouwdienst of Rijkswaterstaat spends 20 million Euros on operation and maintenance of single seal expansion joints, which makes it a large head of expenditure. Therefore it is important to gain insight in the behaviour of various types of expansion joints. In recent years Rijkswaterstaat has paid a lot of attention to single seal expansion joints, because they are applied in over 4000 viaduct structures (Voskuilen et al. 2006).

However there are also major problems related to multiple seal expansion joints. In the Netherlands they are usually applied as modular expansion joints and can be found in long span bridge structures. Modular expansion joints were used for the first time during the sixties. At that time there was a tendency for increasing the spans of bridge structures, as technology developed and balanced cantilever bridges, cable stayed bridges and suspension bridges gained popularity. Consequently this meant that expansion joints had to cope with larger bridge movements. Due to the fact that applying many single seal joints would be very costly, a demand for multiple seal joints arose.
Nowadays there are several manufacturers with their own variations in design to the basic concept for modular expansion joints. Depending on the design, in the extreme situations gaps between the abutment and superstructure of 5000 mm can be spanned with dilatations of 2400 mm, but for most joint designs translations of 1000 mm are a maximum value.

1.1. Problem definition

As stated before, the basic concept of modular expansion joints consisting of centre beams supported by crossbeams is over 30 years old. Current design and construction is based on many years of experience and often simple modelling. The joints however have a strong 3D-behaviour. This in combination with the unpredictable character of road traffic requires computer models in order to enable accurate predictions on dynamic and fatigue behaviour, and fatigue lifetime calculations. Also aspects as, for example, uncertainties and inaccuracies in execution with regard to the required prestress levels of sliding springs, see Figure 2.8 and Table 2.1, make predictions on the behaviour difficult. Loss of prestress can cause the sliding bearings to dislocate, which changes the overall behaviour of the joint system.
Recent graduation works at TU Delft on modular expansion joints, Steenbergen (2003) and Pijpers (2005), focused on joints made by the German company Maurer Söhne. For historical reasons, many bridges in the Netherlands are equipped with these expansion joints. Another German company that produces modular expansion joints is Sollinger Hütte. Their "WSG Lamellen-Dehnfuge" was subject of analysis during this graduation work.

This research has been performed to obtain a better understanding of the structural behaviour of WSG-type modular expansion joints. This concerns not only the behaviour under static loading, but especially the behaviour under dynamic and fatigue loading, because these are important for risk of premature failure of the structure. Another objective was to produce a three-dimensional finite element model, because for current design simple two-dimensional line models and 'Überrollversuchen' (over-rolling test) are used to determine the dynamic behaviour. The 3D-analyses of this model will indicate parameters suitable for optimisation and by doing so the structural behaviour can be improved.

The finite element analysis program MIDAS/Civil has been used to model the three-dimensional behaviour of the structure under the different loadings. There is also a more practical application that adds value to the use of analysis programs besides the possibility to get a better three-dimensional behaviour. As the perfect situation does not occur due to uncertainties during design phase and inaccuracies in execution, reality never corresponds with the design drawings one on one. Usage of analysis software allows for alteration of variables and comparison of their influence.

1.2. Definition of the thesis subject

The description of the problem leads to the following definition for this research:

A study into the structural behaviour of modular expansion joints of Sollinger Hütte.

1.3. Research scope

In order to reach the objectives several different steps have been undertaken. These steps are in short summarized below to give a quick overview of the contents of the research:

- A literature study has been performed concerning the following aspects:
  - Product families of expansion joints;
  - The most important manufacturers of modular expansion joints and their products;
  - Construction and functioning of the Sollinger Hütte WSG Lamellen-Dehnfuge;
  - Regulations that apply for modular expansion joints;
  - Joint movements and the different load situations;
- The expansion joint of bridge Heteren functioned as a case-study for this bridge is equipped with several WSG-type joints;
- In May 1999, the calculations for the joints for Bridge Heteren were made by using the Bouwdienst standard NBD-00710. In the mean time Eurocodes are more and more applied when making design calculations. For expansion joints a technical approval guide is under development that is based on the Eurocode loads. With the use of this document an analytical calculation is made. The results were compared with the original calculations;
- A WSG-type expansion joint was modelled with the finite element program MIDAS/Civil;
- Dynamic and fatigue calculations were performed with the numerical software. These calculations finally resulted in values for relevant dynamic factors;
- The outcome of the numerical calculations have been compared with the results of recent experiments by Sollinger Hütte on the same type of joint in Germany.

Boundary conditions
That expansion joints are available in so many different forms and sizes follows from the fact that there are many applications where they can be used. Expansion joints are applied in buildings, road and rail bridge structures. This research focuses only on expansion joints located in bridges loaded by road traffic. Although road bridges can be made of different materials there is no need to make a distinction between concrete bridges or steel bridges, because the Sollinger Hütte modular expansion joint can be applied for both types of construction materials as can be seen in Appendix II.

With regard to the loading condition of the expansion joint under consideration, some boundaries are applied in this study. During this research only normal loading conditions have been considered. Exceptional loading, like collision forces on kerbs or seismic loading is beyond the scope of this research.
Pijpers (2005) shows in research on Maurer D320-joints that there are various models available to represent the distribution of the contact pressure over the wheel length. Here, a uniform load distribution over the width of a wheel print is assumed in accordance with the Ostermann-model.

1.4. Structure of the report

Chapter 2 describes the different types of single and multiple seal expansion joints and the major manufacturers of modular expansion joints. In the next chapter, a more elaborate description of the modular expansion joint by Sollinger Hütte follows together with a description of bridge Heteren which functions as a case-study in this research.
In chapter 4 attention is given to the various national and international regulations applicable to expansion joints. Followed by the actions of bridges and the loads acting on them in chapter 5. Then in chapter 6 the assumptions and results of the analytical calculations based on Annex G of ETAG No 32 are presented.
Chapter 7 and 8 are addressed to the pre- and post-processing phase of three-dimensional numerical analysis. First the finite element model of the WSG-joint and the choices made concerning the analysis are discussed. The results of the analysis are presented in chapter 8. Finalising the research conclusions and recommendations are presented in the last chapter.

2. Expansion joints

In this chapter expansion joints will be described more in detail. First some more information will be given on the functioning and the different joint types that exist. In paragraph 2.2 and 2.3, respectively the different single and multiple seal joint types will be described. Last in paragraph 2.4 attention will be given to the manufacturers that are the main players on the market for the production of modular expansion joints.

2.1. General

Expansion joints have to fulfil a number of requirements in order to function properly. The main requirements are:

- Provide a smooth transition between the abutment and the superstructure of the bridge for traffic to pass;
- Take up the expansion and contraction movements of the structure;
- Provide water tightness in order to protect the bearings and substructure from water, de-icing salt and debris.

With the increase of traffic flow and heavier loaded trucks since the middle of the nineties emission of noise has become an important design issue too. Since many highways in the Netherlands are located in urban areas, silent operation has become a more important requirement for expansion joints. A joint's lifetime also has become more important, since maintenance often leads to interruption of traffic and consequently results in traffic jams.

When a choice for an expansion joint has to be made, quite a number of solutions are available with each their own benefits and disadvantages. Although designs may vary slightly per manufacturer there are many similarities in joint types. Both national and international (Leendertz and Van der Ven, 2006; EOTA, 2006) seven types of joint families are recognized in order to enable a distinction between the different forms of expansion joints. The seven types are as follows:

1) Buried joints;
2) Flexible plug joints;
3) Nosing joints;
4) Mat joints;
5) Cantilever joints;
6) Supported joints;
7) Modular joints.

The first types of joint families (no. 1 and 2) can only take care for small or medium sized movements of the bridge. These joints have only one rubber seal. Modular joints belong to the category of multiple seal joints together with some of the supported joints. However, there is also a group of supported joints that belongs to the single seal joints.

The single and multiple seal joints will be described more closely in the following two paragraphs. Besides the structural behaviour and range of dilatation gap dimension also known problems will be discussed for each type of expansion joint.

2.2. Single seal joints

Six out of the seven types of expansion joint families (no. 1 - 6) belong to this category, making it the group of joints with the largest diversity in product design and application. Therefore within this category a distinction can be made between joints for small and medium movements.

2.2.1. Joints for small movements

Two types of joint families form this subcategory, i.e. the buried joints and flexible plug joints. These expansion joint types can handle movements up to 30 mm.

Buried joints
By means of this expansion joint a continuous asphalt surface layer can be constructed with a supporting element covering the gap, Figure 2.1. Movements are transferred equally to the pavement through shortening or extension of the supporting element. Depending on the thickness of the surface layer horizontal movements up to 10 mm are possible.
Known problems for this type are cracks in the joint element and fraying of the asphalt surface. Also the water tightness is disputable and therefore an additional sealing is recommended. The joint has a low noise emission.

Flexible plug joints
This type has a flexible mass above the joint, which is a specially modified asphaltic material and a metal plate covering the gap. An impression of the joint is given in the right part in Figure 2.1. The flexible mass allows for dilatations up to 30 mm by means of shortening and extension.
Some of the disadvantages are cracks in the joint, movement of the plate, susceptive to development of wheel tracks and disconnection of the asphaltic material. However the joint can be replaced quickly.

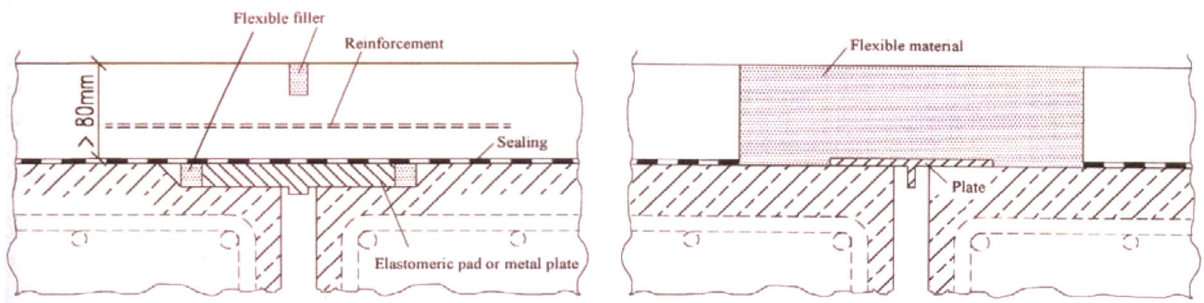

Figure 2.1 Left: Buried expansion joint; Right: Asphalt plug joint.

2.2.2. Joints for medium movements

Expansion joints belonging to this subcategory can take up movements over 25 mm and roughly up to 100 mm, although some types even can provide for dilatations up to 440 mm depending on the manufacturer.

Nosing joints
For this joint family there is a large diversity in products available. A common design for a nosing joint, which for example Bouwdienst Rijkswaterstaat uses in case of new projects, is shown in Figure 2.2. The joint consists of steel or aluminium nosings, which carry the traffic loads, and a rubber seal element. The sealing element provides for water tightness, dilatation up to 100 mm and relative movements of 40 and 10 mm in respectively transverse and vertical direction.
Effectiveness of nosing joints is dependent on factors as nature of the design and materials, workmanship and condition of the substrate at installation (Lee, 1994). As a result problems such as loosening of the anchorage, corrosion of steel nosings and leakage occur. Also noise emission is an issue with these joints and requires extra measures.

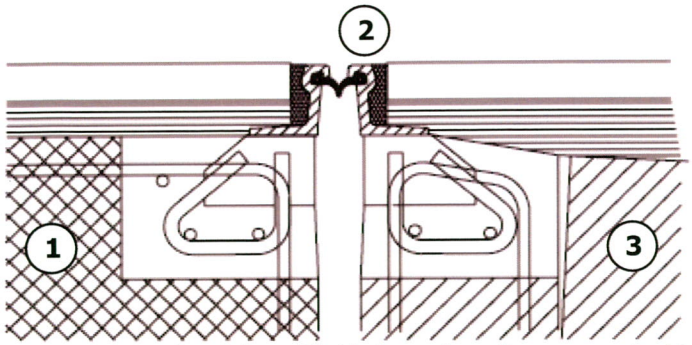

No.	Components
1	Bridge deck
2	V-shaped sealing
3	Abutment

Figure 2.2 Nosing joint with V-shaped sealing connected to a concrete deck system.

Mat joints

Within the family of mat joints a distinction can be made between two groups. The first group, left picture in Figure 2.3, takes up movements by means of extension and shortening. The second group, the picture on the right, does it by means of shear deformation. Depending on the specific product, longitudinal movements up to 160 mm can be accommodated.
Some products belonging to the family of mat joints perform very well and need little maintenance and repair, while others have problems concerning water tightness, loosening of the bolted connection or cracks above the vulcanised steel profiles.

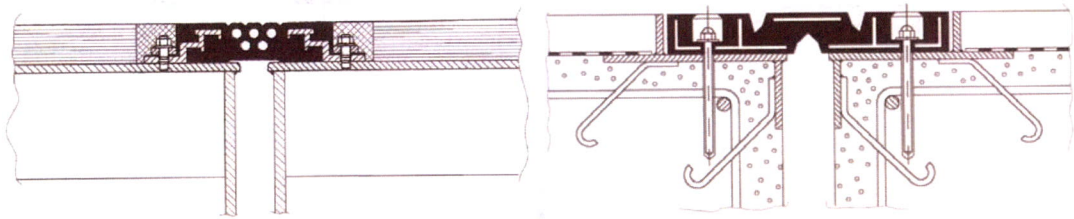

Figure 2.3 Examples of the two different kinds of mat joints.

Cantilever joints

This type of joint family is also known as steel finger joints, because of the cantilevering fingers that grab into each other. The joint is a very robust construction and allows for dilatations up to 440 mm. However movements in transverse and vertical direction are limited and can prejudice traffic safety. Fatigue damage of anchorage and accumulation of debris due to the open character of the joint are problems that can occur. Additional systems are needed to provide for water tightness and reduce the noise emission.

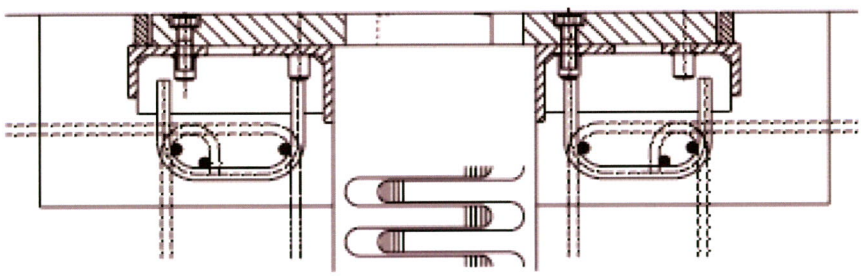

Figure 2.4 Cross sectional view and detailed top view of a steel finger joint.

Supported joints

These joints have a close resemblance to the cantilever joints. An example of a supported joint is given in Figure 2.5. The rectangular plates are rigidly connected at one side and slides over the other end. The joint can be connected by means of a hinge or with a certain rotational stiffness at the location of the rigid support. Depending on the design of a supported joint dilatations up to 250 or even 1000 mm are possible. Similar to cantilever joints transverse and vertical movements are limited. In the Netherlands supported joints have not been applied. However, Rijkswaterstaat has its doubts about the durability of (certain components) of this type of expansion joint.

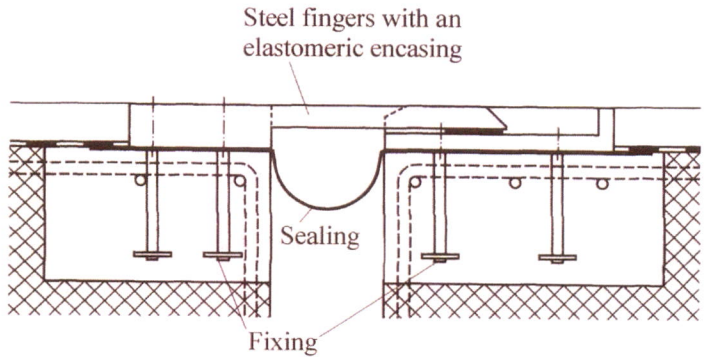

Figure 2.5 Finger joint with supported fingers.

2.3. Multiple seal joints

As mentioned in the first paragraph of this chapter, the category of multiple seal joints consists of modular expansion joints and one kind of supported joint.

2.3.1. Rolling leaf joint

Also known as roller shutter joints or Rollverschluss Fuge (Germany), rolling leaf joints belong to the family of supported joints. In the last decennia rolling leaf joints have been improved with regard to water tightness, noise emission and structural behaviour. An impression of the joint is given in Figure 2.6.
Longitudinal movements up to 2 meters are possible by means of sliding plates that are placed in series and fixed at one end. Rubber seals are placed between the plates to prevent leakage.
Although the concept of the joint has been improved problems occur concerning cracking of anchors, springs and hinges between plates due to fatigue and wearing of sliding elements.

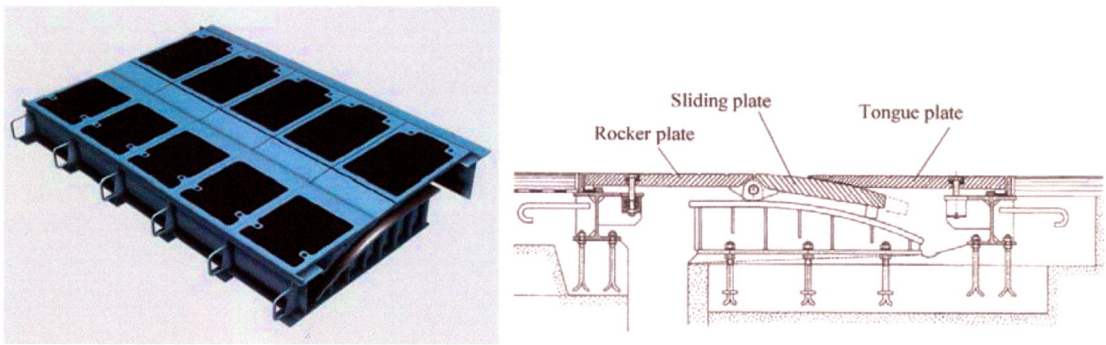

Figure 2.6 3D view and cross sectional view of a rolling leaf joint.

2.3.2. Modular expansion joints

The basic concept of modular expansion joints is a series of steel beam profiles, called centre beams, in transverse direction of the bridge that are supported by support bars. The support bars rest on both the bridge deck structure and the abutment. The centre beams are kept at equal distances by means of control elements. Between the centre beams rubber seals are placed to provide for water tightness. Modular expansion joints can be used for steel as well as concrete bridge structures. The three variants of modular expansion joints available are shown in Figure 2.7.

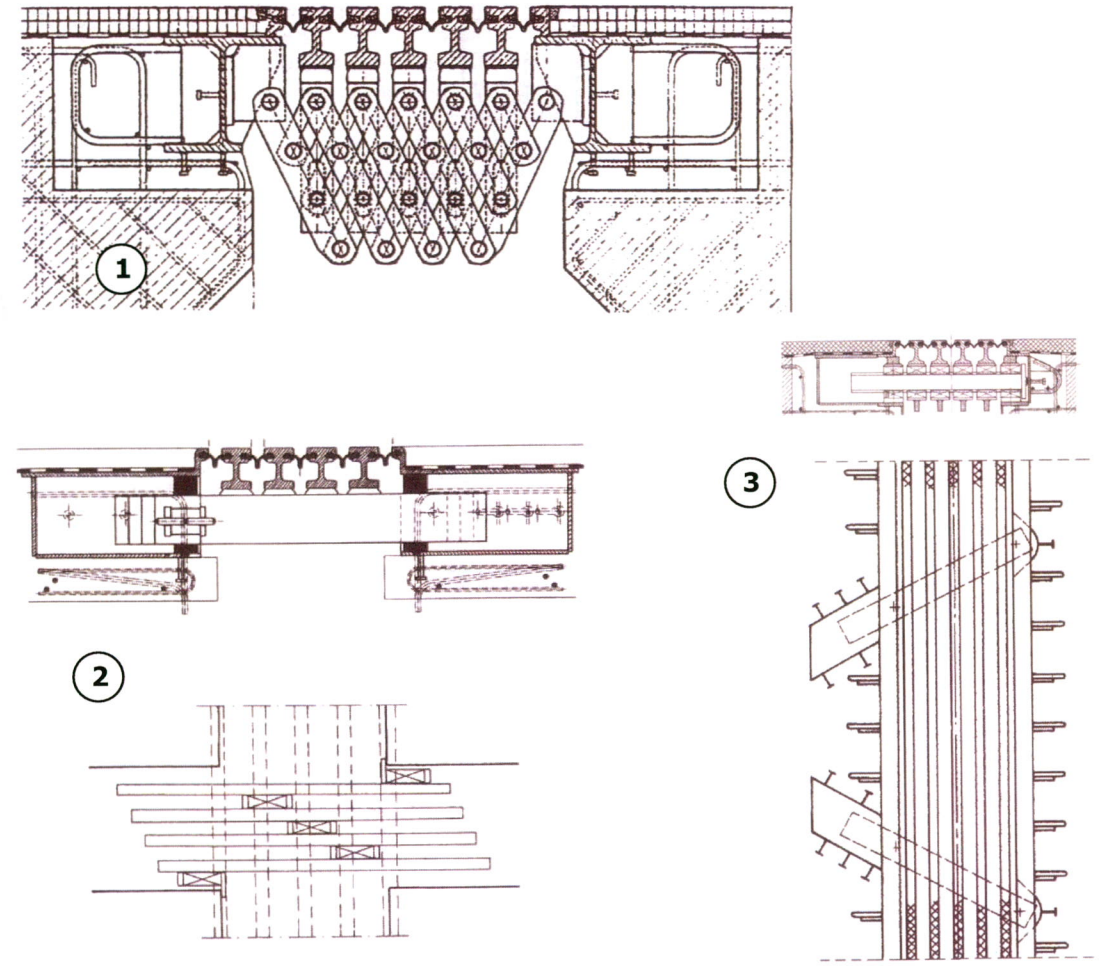

Figure 2.7 (1) Mechanical support system or "Lazy-tong' expansion joint;
(2) Multiple-support bar system; (3) Single support bar system.

For a multiple-support bar system the support bars next to each other, carry only one centre beam each. This kind of linkage system has the disadvantage that forces caused by braking and acceleration result in non-uniform spring deformations. If a gap is opened near to the maximum value the seals can be over expanded. Figure 2.8 shows a three-dimensional view of a multiple-support bar system and in Table 2.1 the functions of the different elements corresponding to the numbers, are given.
In case of a single support bar system the bars can be placed in a skew position, Figure 2.7 lower right. In such a joint the gap width is controlled by means of the kinematic characteristic of the mechanism. The support bar can rotate around the horizontal level on both sides, but only at one side it can translate in a direction with an angle to the moving direction of the bridge structure.

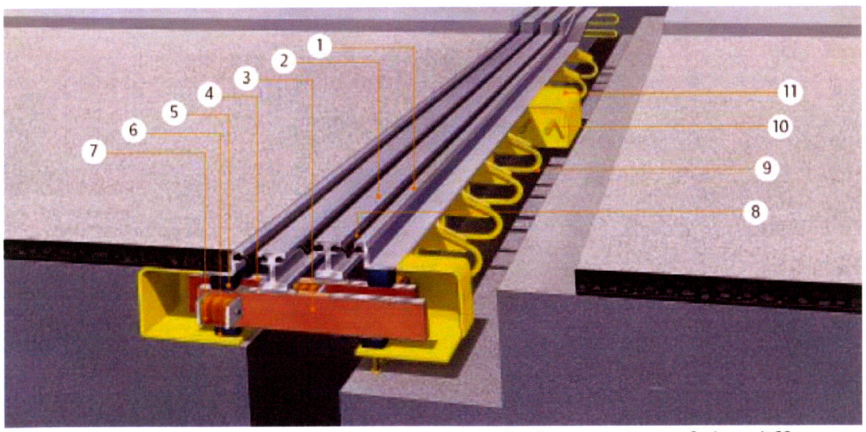

Figure 2.8 Multiple-support bar system with designation of the different elements.

Table 2.1

No.	Element name	General function
1	Edge beam	Supporting element. Usually hot-rolled or welded built-up sections of construction steel.
2	Centre beam	
3	Support bar	
4	Sliding plate	Support. The elements have sliding surfaces of austenitic steel sheets and of polymer materials like PTFE or POM.
5	Sliding spring	
6	Sliding bearing	
7	Control spring	Control element. Made of an elastic material.
8	Strip seal	Sealing element. Made of enhanced rubber.
9	Carriageway anchor	Anchorage.
10	Anchor stud	
11	Support box	

Independent of the support system that is applied or the producer chosen, several general problems arise during the lifetime of modular expansion joints. Common problems are aging of the strip seals, leakage due to damaged or insufficiently cleaned seals, corrosion of steel components and aging and/or wear of prestress and control springs.

2.4. Producing companies

In this paragraph four of the main manufacturers with their different types of modular expansion joints are discussed. However it is not intended to give a complete overview of all companies that operate worldwide.

2.4.1. Mageba

The Swiss manufacturer Mageba is an international operating company providing products for the civil engineering industry such as bridge bearings, shock absorbers and expansion joints. Besides several different types of single gap joints, they produce one type of modular expansion joint.

Tensa Modular Type LR

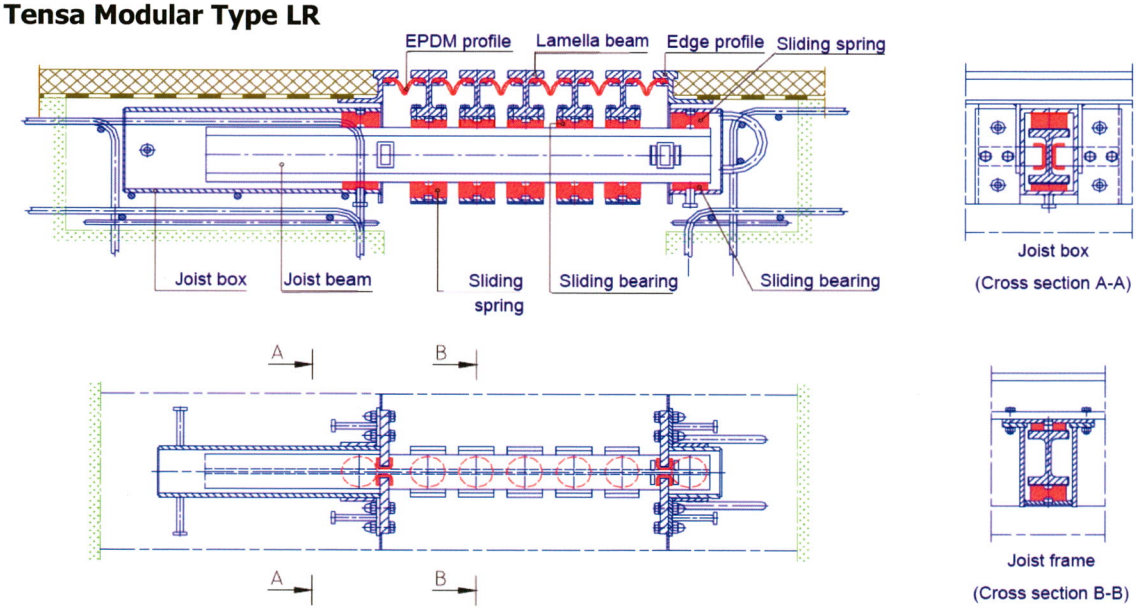

Figure 2.9 Different cross sections of the support bar and the connection between the support bar and centre beam of a Mageba LR joint.

The Tensa Modular Type LR expansion joint is a single support bar system where support bars are placed perpendicular to the centre beams. Every centre beam is supported by each support bar with the use of a joist frame, see Figure 2.9, which is connected to the centre beam by means of prestressed bolts. Prestressed elastic sliding elements allow the frames move along the support bars. Each support bar is supported at one side in a similar way allowing the bar to slide in and out of the support box.
Optionally the expansion joint can be equipped with sinus plates, which reduce the noise generated by traffic. The noise is reduced because there are no straight edges perpendicular to the traffic direction anymore. For areas with risk of earthquakes the expansion joint can be equipped with a so-called Fuse-Box, which protects the joint and adjacent structure from damage and ensures that emergency vehicles still can cross the structure after an earthquake.

The Type LR modular expansion joint allows for dilatations ranging from 160 till 2400 mm in the traffic direction of a bridge. Movements in transverse direction of 12 mm and vertically of 21 up to 32 mm are possible for this joint type.
Bridge projects in the Netherlands where this type of modular expansion joints has been installed are the Maarsserbridge, the Dintelhaven Bridge near Rotterdam and the Kreekrak bridges.

2.4.2. Maurer Söhne

With its main office in Munich, the German company Maurer Söhne GmbH & Co. KG operates in over 50 countries. In Europe it is one of the leading companies for the production of bridge bearings, expansion joints and seismic devices for bridges and civil engineering.
With regard to expansion joints Maurer Söhne manufactures both single seal and modular expansion joints. For modular expansion joints they have three solutions available, which will be given attention hereafter. For a more elaborate description of their functioning see Pijpers (2005).

Girder grid expansion joint
The modular expansion joint shown previously in Figure 2.8 is in fact a Maurer girder grid expansion joint. The girder grid expansion joint or 'Trägerrostfuge' (German) is a multiple-support bar system. At the location of a support box each separate centre beam is welded to a separate support bar. The support bars can slide in and out of the support boxes at one or both edges of the structural gap. In between the centre beams V-shaped rubber seals ensure the water tightness of the structure.

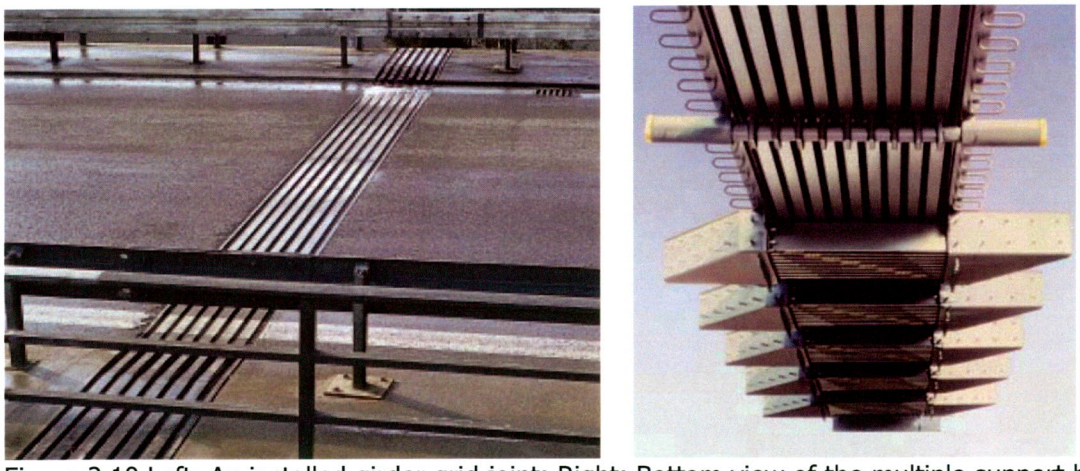
Figure 2.10 Left: An installed girder grid joint; Right: Bottom view of the multiple support bars.

In the current product design 2 up to 8 rubber seals are used, which means that dilatations varying from 160 to 640 mm can be achieved. Depending on the size of the girder grid joint relative movements of 10 to 20 mm in transverse direction and of 20 to 80 mm in vertical direction can be achieved.
This modular expansion joint has been used for various bridges in the Netherlands. Some examples are the Hagestein bridge, the Martinuss Nijhoff bridge and the 2nd Stichtse bridge.

Swivel joist expansion joint
The 'Schwenktraversen-Dehnfuge' or Swivel joist expansion joint is a single support bar system with its support bars in a skew position, as is illustrated in Figure 2.11. How this system functions has already been described in paragraph 2.3.2.
Different from the girder grid joint a stirrup is welded to a centre beam in order to connect the beam to the support bar. Prestress and sliding elements between the stirrup, the centre beam and the support bar allow translations and rotations along the support bar.
Similar to the Type LR joint by Mageba, the Swivel joist expansion joint can be equipped with a fuse-box when it has to be installed in seismically endangered structures. It can also be produced as a XL expansion joint, which will discussed next.

The fact that all centre beams are supported on one support bar makes that the Swivel joist joint can accommodate much larger movements than the girder grid expansion joint. Depended on the type applied movements of 160 mm up to and even over 2 m are possible in traffic direction. Also larger movements in the two spatial directions perpendicular to the traffic direction are possible. Movements of 80 to 1000 mm in transverse direction and 10 to 45 mm in vertical direction can be accommodated.

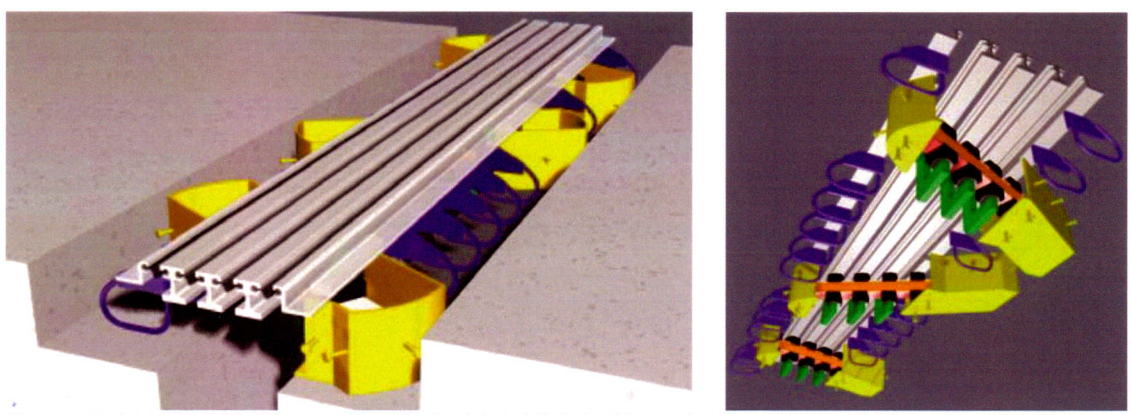
Figure 2.11 Left: 3D view of the Swivel joist joint; Right: bottom view of the support bars.

In the Netherlands this expansion joint has been applied in the Herman de Man Bridge across the Waal River near Ewijk. This type has also been used for the Storebaelt East Bridge in Denmark and the Vasco da Gama in Portugal.

XL expansion joint
This is in fact a redesign of the girder grid expansion joint. The joint is equipped with rhombic steel plates, see Figure 2.12, which due to their geometry make it possible to have a maximum single gap opening of 100 mm compared to the common maximum value of 80 mm. However the main function of these rhombic steel plates is to provide a reduction in the emission of noise and they also act as a protection against snowploughs. XL expansion joints have been applied in many road bridges in Germany and Austria.

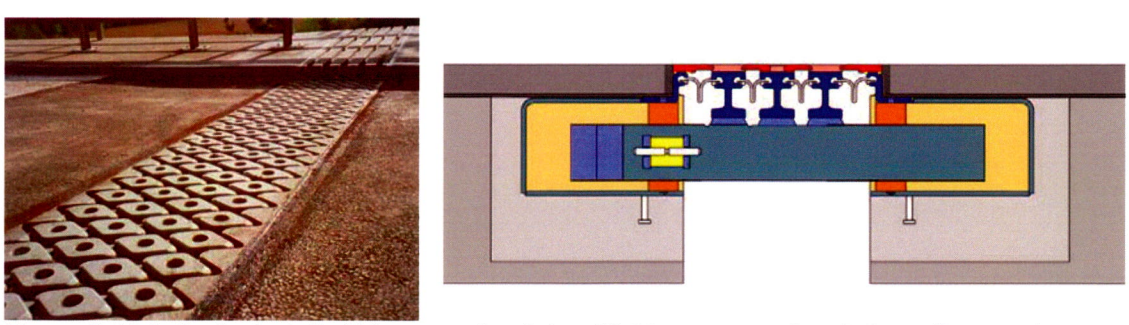
Figure 2.12 Left: An installed XL expansion joint; Right: cross sectional view of a crossbeam.

2.4.3. Sollinger Hütte

Founded in 1715 as a foundry and metal construction business, RW Sollinger Hütte GmbH nowadays is focused on the development, production, installation and repair of bearings and expansion joints for bridges and buildings. The company's office and factory are located in Uslar, Germany. Although Sollinger Hütte produces several types of expansion joints, it only has one type of modular expansion joint.

WSG-type girder grid joint
This modular expansion joint can provide dilatations ranging from 160 to 1200 mm, see Appendix II. Relative movements in transverse direction of about 20 mm and in vertical direction of 10 mm are possible.
Some examples of bridges where the WSG-type joint has been applied are the Etzelsbach Valley Bridge in Thuringia, the Rodenkirchen Bridge in Cologne and the Panyu Bridge in Guangdong, China.

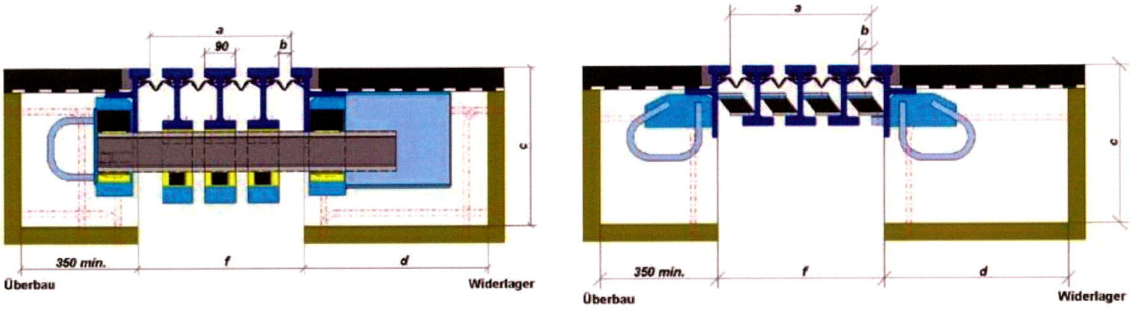

Figure 2.13 Left: Cross sectional view of a crossbeam of a WSG joint;
Right: Cross sectional view of the control system.

Similar to the Tensa Modular Type LR by Mageba, the WSG joint is characterized by a stirrup construction for the connection between the centre beams and the support bars. Also here the connection is achieved with bolts. A more elaborate description of how the joint is built up and how the construction functions will be given in paragraph 3.1.

Besides a technical approval for this type of girder grid joint in accordance with TL/TP-FÜ 92 in its home country Sollinger Hütte also has technical approval for this product in Austria where it satisfies RVS 15.45. In paragraph 4.2 the concept of the technical approval system will be given attention.

2.4.4. Watson & Bowman

The core activities of the American company Watson Bowman Acme Corporation are focused in the area of production of expansion control systems for civil engineering. This involves not only manufacturing expansion joints for buildings and bridge structures, but also the production of products for corrosion protection, sealing elements, etcetera. For bridge structures Watson Bowman can deliver two different products, which are very similar to the joints by Maurer Söhne.

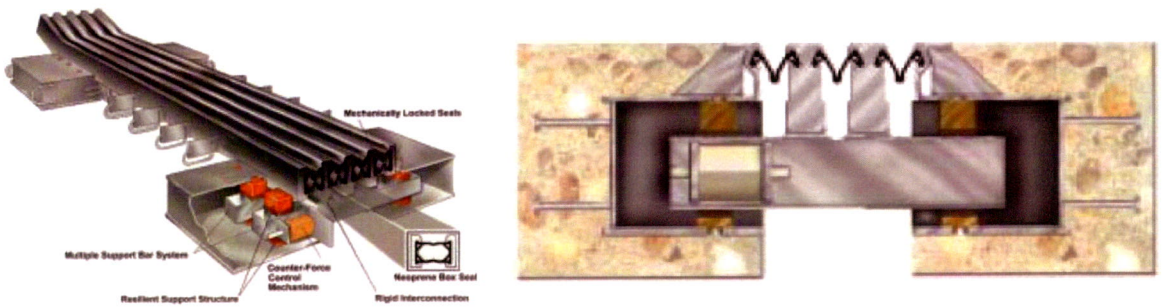

Figure 2.14 Left: 3D view of the Modular D joint; Right: Cross sectional view of a crossbeam.

Wabo Modular D or STM joint
For this multiple-support bar system the connection between the centre beams and support bars is achieved by means of welding. The Wabo Modular joint can be equipped either with neoprene box seals (D-joint) or with V-strip seals (STM-joint), see Figure 2.14.
One could state that a box seal is more advantageous, because it provides additional horizontal stiffness to the structure and extra safety regarding the water tightness due to the two layers. However if cracks occur in the top layer of the seal, water can accumulate and when the seal freezes the seals will break and loose its function.
The Wabo modular expansion joint has a total movement capacity ranging from 150 to 760 mm.

Wabo X-cel modular joint
This expansion joint is a single support bar system, where the support bars are placed perpendicular to the centre beams as illustrated in the figure below. The X-cel joint allows for structural movements in all directions. The longitudinal movements are accommodated within the longitudinal box while transverse movements are accommodated by transverse boxes. Different from other modular expansion joints, the X-cel joint is not equipped with an elastic spring mechanism for controlling the equal spacing of the centre beams. Instead movements are controlled by means of a kinematical system that rotates around a fixed point.

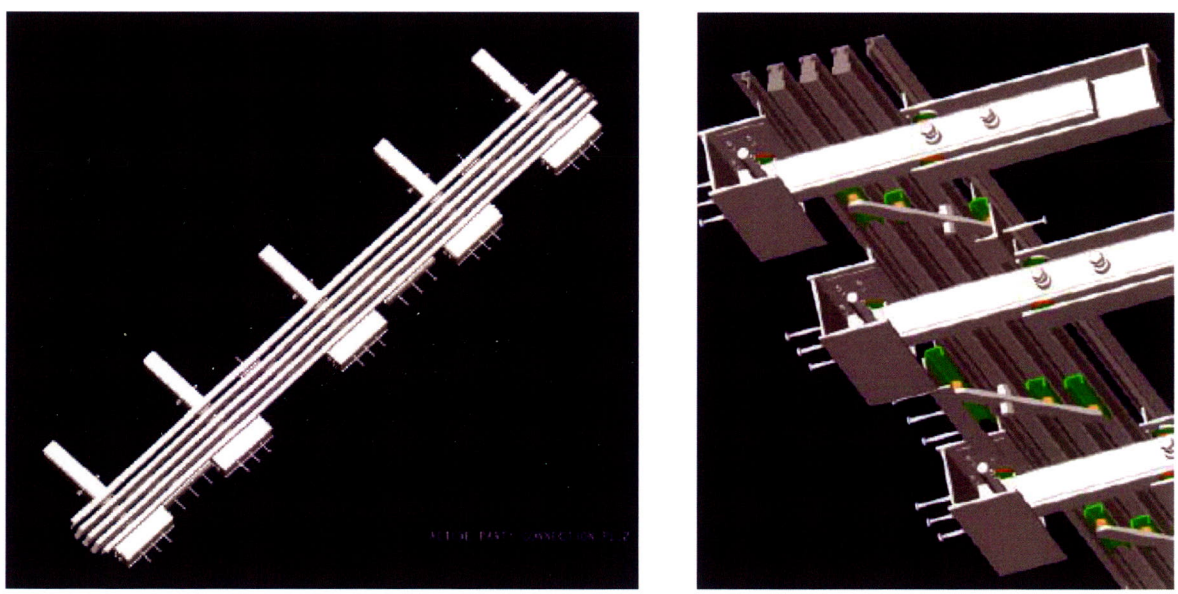

Figure 2.15 Left: Top view of the X-cel joint;
Right: Bottom view of the support bars and control system.

3. Sollinger Hütte Type WSG joint

In the previous chapter a short description has been given of Sollinger Hütte GmbH and WSG-type the modular expansion joint they manufacture. The first paragraph of this chapter goes in more detail into the structure of the expansion joint and how it functions. After this bridge Heteren is described as the joints in this bridge function as a case-study during this research.

3.1. Composition and operation

The WSG type modular expansion joints made by Sollinger Hütte are built up out of centre beams and crossbeams, Figure 3.1, and have a so-called "Trägerrooststruktur" or girder grid system. This means that the support bars are placed perpendicular to the centre beams and each support bar carries all centre beams. This makes it a single-support bar system.
The structure is controlled by means of control springs which ensure that the centre beams remain parallel to and at equal distances from each other and the edge beams. The springs also contribute to the horizontal stiffness of the system. The centre beams are able to move over the support bar by means of stainless steel sliding plates when the horizontal traffic force is large enough to overcome the friction.

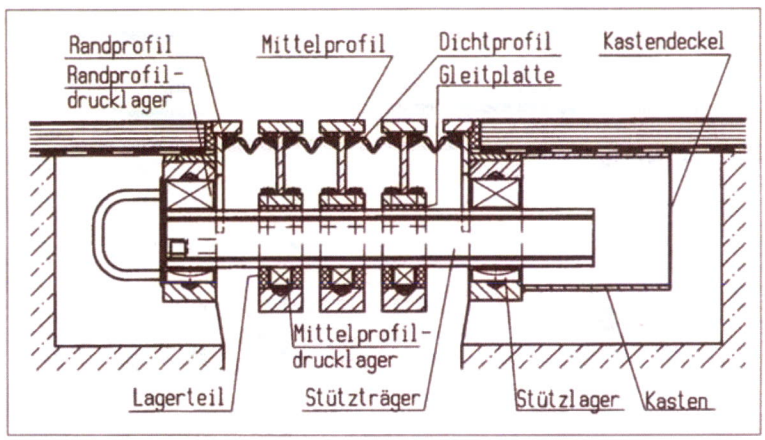

Figure 3.1 Cross section of the support bar with designation of the different elements.

German	English
Randprofil	Edge beam
Mittelprofil	Centre beam
Stützträger	Support bar
Gleitplatte	Sliding plate
Dichtprofil	Strip seal
Lager	Bearing
Steuerfeder	Control spring
Bügel	Stirrup
Schraub-verbindung	Bolted connection
Betonanker	Carriageway anchor
Kasten	Support box

Centre and edge beams
Formed by welding S355 plate elements together, centre and edge beams are the main parts of the expansion joint. They are placed perpendicular to the traffic direction and the top surface of the upper flange is located at the same level as the surface of the road pavement.

Support bar
As stated before, the support bars bear all the centre beams and transfer the vertical traffic loads to the support bearings. Also part of the horizontal forces that is not taken up by the control elements is transferred by friction from the centre beam to the support bars.
A support bar is simply supported on the bearings located in the support boxes. This means that at one side movements in the three possible directions are prevented and at the other end the bar can slide in and out of the box only in longitudinal direction. Free rotation of the bar is not obstructed by the bearings at either side.

Bearings
Structural elements are supported by bearings, which transfer the loads to the foundation or other elements. They also allow or limit the degrees of freedom of the structural element. In the WSG-joint three different kind of bearings can be recognized. In Figure 3.1 all three can be seen:

- The support bar bearings (Stützlager);
- The compression bearing between support bar and edge beam (Randprofildrücklager);
- The compression bearing between support bar and stirrup (Mittelprofildrücklager).

The support bar bearings are produced from polyamide (PA) which is a kind of plastic. When a bearing is placed in the construction it will adjust itself to the correct position. At one side it is equipped with a stainless steel plate to allow the support bar to slide. The support bar bearings can not take up tension forces. Therefore the compression bearing on top of the support bar is given an initial prestress. This rubber block also contributes to the minimization of noise emission.
The third type of bearing mentioned, see also Figure 3.3, is made of PTFE and Polyoxymethylene (POM) which is a very rigid plastic. This bearing contributes to the transfer of the loading from the centre beams to the support bar and to the sliding of the centre beam over the support bar.

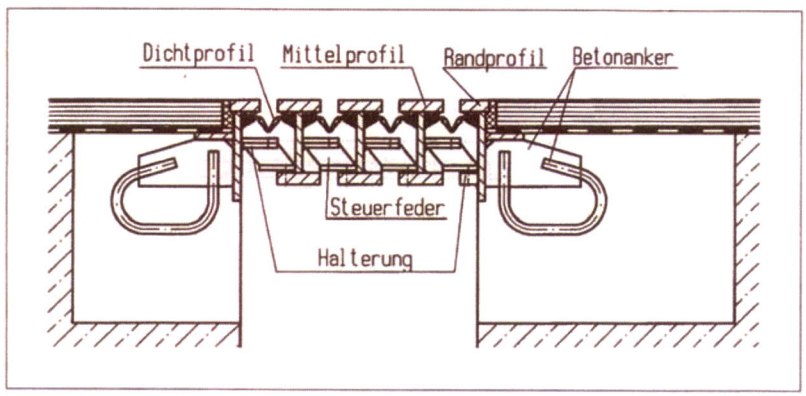

Figure 3.2 Cross section of the control system with designation of the different elements.

Control springs
These elements have an important role in the movement behaviour of the structure. The control springs are built up out of two S235 steel plates with in between a parallelogram shaped CR-rubber block, see Figure 3.2. By means of vulcanisation the plates are connected to the rubber. The connection of a plate to a centre beam or edge beam is made with bolts.
The rubber elements contributed in several ways to the structural behaviour. First of all, they ensure the equal and parallel spacing between the centre beams and between the centre and edge beams. Secondly, due the arrangement close to the road surface the eccentricity moment arising from braking and acceleration forces are limited. The rubber blocks also take up part of the torsion moment caused by the eccentricity of the vertical loads.

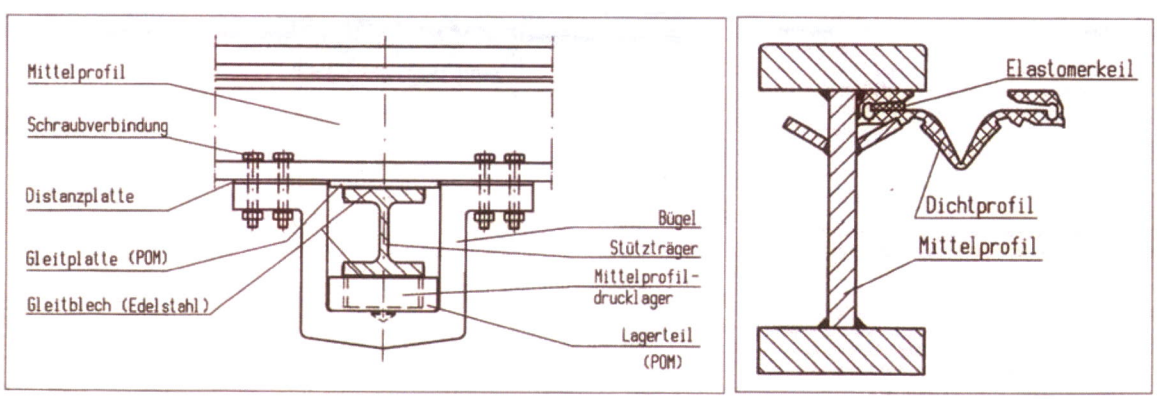

Figure 3.3 Left: Cross section of the connection between the support bar and a centre beam;
Right: The rubber profile is kept in place by means of wedges.

Rubber sealing
The V-shaped rubber seals provide for water tightness and in this way protects the underlying construction. The V-shape ensures that the seal is not damaged by small pebbles when the joint is completely closed. The seals are resistant to climate influences like UV-light, ozone, de-icing salts, oil and most chemicals that are being transported over the road. The right part of Figure 3.3 shows how the seals are locked in between the flanges of a centre beam with the use of rubber wedges.

Connection between centre beam and support bar
The way how this connection is achieved characterizes this modular expansion joint and gives it several advantages in respect to other concepts. The connection consists of a stirrup element that is connected to the centre beam with 8 bolts. This is shown in Figure 3.3. It is essential that the bolts are prestressed in order to have a high fatigue detail classification at this location in the centre beam. The advantage of a bolted connection is the absence of residual tensile stress, as will be explained in paragraph 5.2, which have a negative influence on fatigue life of a cyclic-loaded structure.

This type of connection has several other advantages, such as:
- The bolts can be loosened from the underside of the structure;
- Easy replacement of every single element of the connection;
- Insusceptibility to imposed deformations;
- Reduction of the noise emission due to the prestressed bearing.

The stirrup connection also contributes to preventing lateral buckling of the centre beams.

3.2. Bridge Heteren

The bridge across the river Rhine near Heteren is the one of the two bridges in the Netherlands where WSG-type expansion joints of Sollinger Hütte are applied. A short historical overview of this bridge will be given.
In 1969 construction of Bridge Heteren across the river Rhine started. At the time the bridge was constructed as part of national motorway no. 75. Nowadays the road is known as the A50 and leads from road junction Hattemerbroek in the north to Eindhoven in the south, see Figure 3.4.
On the 30th of August 1972 the bridge was opened to traffic as part of the 14 kilometre long stretch between road junctions Valburg and Grijsoord.

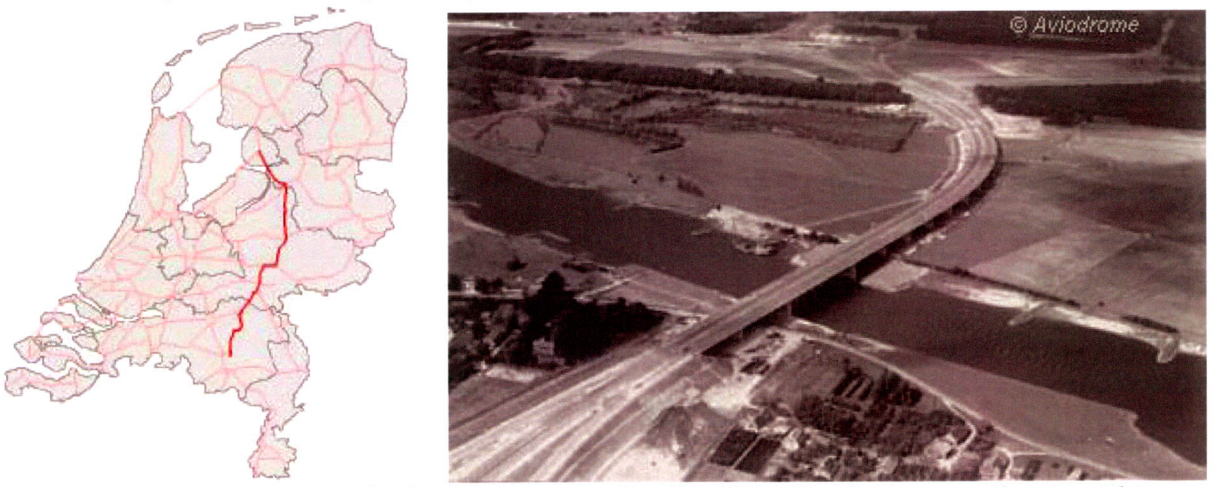

Figure 3.4 Left: Location of Netherlands's Motorway No. 50; Right: The bridge over the river Rhine near Heteren shortly after completion in 1972 seen from the south.

During reparation works in 1999/2000 the old expansion joints in both traffic directions of the bridge where replaced. One WSG 160, two WSG 240's and one WSG 320 modular expansion joint were installed. The choice for expansion joints of Sollinger Hütte was based on the fact that these could be installed on the foundation of the old joints.

4. National and international regulations

For the design, production and installation of expansion joints standards exist on different levels. In both the Netherlands and Germany, requirements exist in addition to the national codes. These standards will be subject of the first two paragraphs. Paragraph 4.3 deals with the European codes for bridge structures and expansion joints. Another European document, a guideline for the design, production and installation of expansion joints, which currently is under development, is described in the last part of this chapter.

4.1. NBD-00710: Requirements for Expansion Joints

In the first chapter it has already been mentioned that the Bouwdienst of Rijkswaterstaat is responsible for the operation and maintenance of the expansion joints in Dutch road bridges. In order to do so the Bouwdienst has developed a series of internal standards in addition to the Dutch standards. For multiple seal expansion joints NBD-00710 (Leendertz, 2006) applies. The requirements in this NBD cover aspect such as dynamic and fatigue design rules, inspection and maintenance.

4.2. Technische Lieferung / Technische Prüfung Fahrbahnübergange (TL/TP-FÜ 92)

In Germany the Ministry of Traffic has a system of so-called 'Regelprüfungen'. With a 'Regelprüfung'-document a manufacturer does not have to show for each project that his product satisfies the national standards. In order to obtain this document for expansion joints, the product has to be tested according to TL/TP-FÜ 92 by a specialized institution, for example a university. When the tests are successful the product is valid for a certain range of dimensions. Now the bridge engineer can easily choose the appropriate expansion joint on the basis of tables with design information. Regelprüfungen are valid for a period of five years after which they have to be reviewed. An example of such a document is shown in the figure below.


FEDERAL MOGUL

SH – Fahrbahnübergang
Typ WSG 160 - 960

Unterlagen mit
Regelprüfvermerk

Regelprüfung nach TL/TP-FÜ 92

gemäß den Anforderungen des:

Bundesministeriums für Verkehr, Bau- und Wohnungswesen
Abteilung Straßenbau, Straßenverkehr, Referat S 25
Robert-Schuman-Platz 1
53175 Bonn

Prüfer:

Dipl.-Ing. Uwe Schmiedel
Fuchsbau 27
D - 25421 Pinneberg

Fremdüberwacher:

Institut für Stahlbau und Holzbau
der Universität Innsbruck
Technikerstraße 13
A - 6020 Innsbruck

Regelprüfung
in statischer und konstruktiver Hinsicht
gemäß TL/TP-FÜ 92
siehe Prüfbericht

Dipl.-Ing. U. Schmiedel, 25421 Pinneberg

FEDERAL – MOGUL SOLLINGER HÜTTE GMBH

Figure 4.1 'Regelprüfung'-document for WSG-type girder grid joints.

4.3. Eurocode

Nowadays European standards, the Eurocodes, are used besides and eventually will replace, the national standards of individual member states of the European Union. For the design and calculations of bridge structures a number of Eurocodes are relevant. A summary of these codes is given in Table 4.1 below.

In most of these Eurocodes expansion joints are not mentioned explicitly. Only Annex E of Eurocode 3 provides some information on the design of several types of expansion joints for road bridges. In the future however this annex will be substituted by a technical approval for expansion joints (ETAG), which will be discussed in the next paragraph.

Table 4.1 Eurocodes with rules for bridge structures.

Title	Description
EN 1990	Eurocode - Basis of structural design
EN 1991, Part 2	Actions on structures – Traffic loads on bridges
EN 1992, Part 2	Design of concrete structures – Concrete bridges
EN 1993, Part 2	Design of steel structures – Steel bridges
EN 1994, Part 2	Design of composite steel and concrete structures – General rules and rules for bridges

Since fatigue failure due to dynamic loading is an issue when designing modular expansion joints, Eurocode 3, part 1-9: Fatigue, is relevant. This part gives methods for the assessment of fatigue resistance of members, connections and joints subject to fatigue loading[1].

4.4. European Technical Approval Guideline

Contrary to bridge bearings (Driessen, 2003) there will be no specific Eurocode concerning design and calculation of expansion joints. Instead ETAG No 32 consisting of 8 parts is currently being developed in order to give guidance on the technical assessment of the fitness for use of expansion joints. This is done by a workgroup of specialists who are in service of government organisations, universities or manufacturers. The workgroup has been given a mandate by the European Commission and when finished their guideline will be adopted by EOTA, which stands for European Organisation for Technical Approvals.

The first part of the ETAG No 32 (EOTA, 2006) deals with the general aspects concerning expansion joints for road bridges and the other parts each deal with one of the seven types of joint families as mentioned in paragraph 2.1.
In view of this master thesis especially Annex G of ETAG No 32 Part 1 - General, is of interest as this annex deals with traffic loads and combinations to be applied in order to check the mechanical resistance.

[1] The definition is taken from EN 1993-1-9, §1.1. (2005).

5. Bridge actions

The road bridge to which it is connected, the road traffic making use of the bridge and thermal actions, influence the behaviour of an expansion joint. The different movements of a bridge will be discussed in the first paragraph. In the second paragraph general information regarding the design and analysis of modular expansion joints will be given and in the last one the traffic loads that have to be considered when designing and analysing an expansion joint are mentioned.

5.1. Movements of bridges

The movements of expansion joints depend on the arrangement of the bridge bearings and are primarily generated by the overall movements of the bridge deck, which are a result of:

- Temperature actions in the bridge;
- External loads, i.e. road traffic;
- Shrinkage and creep in the case of concrete or composite bridges.

With regard to the temperature actions on a bridge a distinction can be made between long- and short-term effects. With the long-term or seasonal effect the variation in temperature of the surrounding environment is meant. This effect causes lengthening and shortening of the bridge structure.
During daytime the surfaces of the bridge structure exposed to the sunlight become much warmer than those on the shadow side and at night the structure losses heat again. The daily (short-term) effect of heating, cooling and difference in surface temperature causes a temperature gradient in both vertical and transverse direction of the deck structure. The figure below shows how these different components influence the temperature distribution over the cross-section of a structural element.

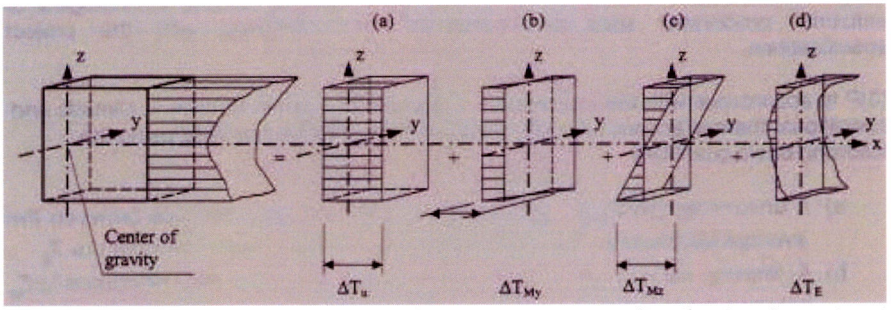

Figure 5.1 Different components of the temperature distribution in a structural element.
(a) Uniform temperature component;
(b) Linearly changing temperature gradient about the vertical axis;
(c) Linearly changing temperature gradient about the horizontal axis;
(d) Non-linear temperature difference component that results in a system of self-equilibrated stresses, which produces no net load effect on the element.

The three actions mentioned, do not only result in translations in longitudinal, transverse and vertical direction, but also cause rotations, see the figure below.

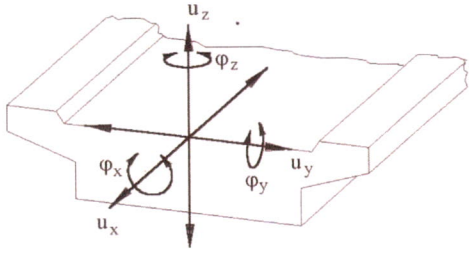

Figure 5.2 Possible translations and rotations about the 3 bridge axis.

Modular expansion joints allow translations in all 3 directions (u_x, u_y, u_z) and rotations about all 3 axes (φ_x, φ_y, φ_z). Movements in the bridge's transverse direction (u_y) and vertical direction (u_z) of both the centre beams and the support bars are made possible due to the elasticity of the support system. For most designs these movements are very small compared to the movement allowed in the longitudinal direction of the bridge (u_x).

5.2. Analysis and design

In the problem definition in paragraph 1.2 it has already been mentioned that current design and construction of expansion joints is based on experience and simplistic calculations.
However a more accurate analysis is very important, because modular expansion joints are sensitive to fatigue.

Ultimate limit state design
Usually performing checks on expansion joints in the ultimate limit state of is done correctly. Practice shows that failure of a modular expansion joint hardly ever occurs due to the fact that the static resistance capacity is exceeded. The verification at the ultimate limit state makes use of a quasi-static approach, where a dynamic amplification is incorporated in the design values.

The static strength safety of structural members is analysed using the semi-probabilistic safety concept, which can be expressed as follows:

$$\gamma_F \cdot S_{Sd} \leq S_{Rd} / \gamma_M$$

In words this means that the lower bound value for the resistance capacity of a member has to be larger than the upper bound value for the loading.

Fatigue design
Although modular expansion joints have functioned quite well in the past premature failure occurred in several situations. Mostly it was a result of fatigue failure caused by poor detailing and/or too large centre beam spans[2]. To the first type belong modular joints having a fillet weld instead of full-penetration weld for the centre beam to support bar connection. The second type was caused by the need for cost-reduction. Increasing the centre beam spans reduced the number of support bars and boxes, but also resulted in larger bending moments and a lower first natural frequency.

Nowadays, the damage observed at modular expansion joints mainly is a result of failure due to fatigue. Three types of fatigue failures, Figure 5.3, can occur (Ramberger, 2002):

1) Fatigue cracks in the welded joint between the centre beam and the support bar;
2) Fatigue cracks in the centre beam;
3) Fatigue cracks in the support bar.

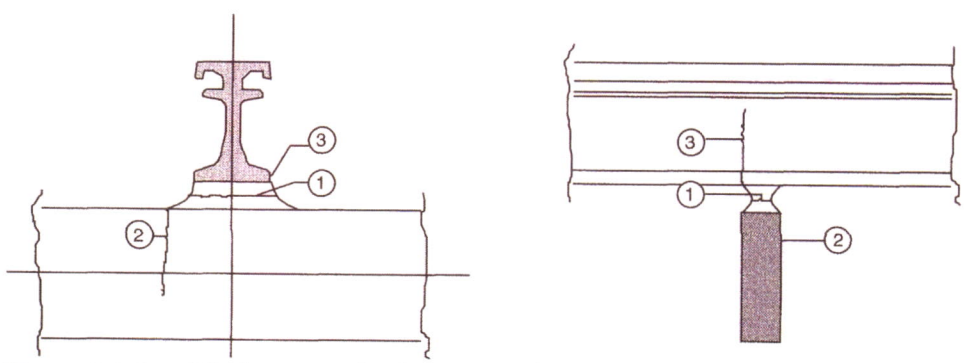

Figure 5.3 Possible locations for fatigue cracks.

[2] Crocetti, R. and Edlund, B (2003). "Fatigue Performance of Modular Bridge Expansion Joints", Journal Of Performance of Constructed Facilities, Volume 17, Issue 4, November 2003, pages 167-176.

The fatigue cracks usually develop in regions of the members subjected to cyclic compressive stresses (type 1 and 2), which are caused by the external loading.
During the welding process there is much heat input in the parent and welding material in order to make a weld with a good quality. When the steel cools down, it wants to contract. By doing so residual tensile stresses come into existence in the material. This is why not the welding process itself, but the physical process afterwards has to be regarded as the reason that cracks occur in and around welded joints.

For fatigue assessment the stress spectrum produced by traffic running on bridges is relevant. The stress spectrum depends on the geometry of the vehicles, the vehicle spacing, the axle loads and the composition of the traffic and its dynamic effects.

5.3. Loads on expansion joints

An analytic verification of the WSG-type joint will be made in chapter 6 based on Annex G of the ETAG No 32 for expansion joints (EOTA, 2006). Therefore the traffic loading as mentioned in this annex will be described.

5.3.1. General

In order to verify the mechanical resistance of bridge structures actual traffic has been simplified and translated into several load models. These models distinguish different zones of an expansion joint, as illustrated in Figure 5.4, to which different loading applies.

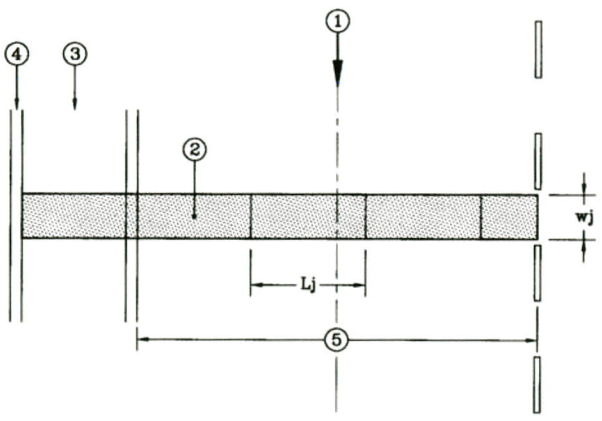

Legend	
1	Traffic direction
2	The expansion joint
3	Footpath
4	Pedestrian parapet
5	Traffic lane

Figure 5.4 The structural length L_j and width w_j of an expansion joint.

The load models make use of axle loads for which the Eurocode uses so-called notional lanes. The number of notional lanes into which a traffic lane can be divided can be determined with the table below.

Table 5.1 Number and width of notional lanes.

Carriageway width w	Number of notional lanes	Width of a notional lane w_l	Width of the remaining area
w < 5,4 m	n_l = 1	3 m	w - 3 m
5,4 m ≤ w < 6 m	n_l = 2	w/2	0
6 m ≤ w	n_l = Int (w /3)	3 m	w - 3 * nl

5.3.2. Vertical wheel loads

These vertical loads are based on the values of characteristic Load Model 1 from EN 1991-2. The wheel print and configuration of tandems to consider are the same as defined in this model. They depend on the structural length and width of the joint. Therefore the appropriate wheel/axle loads and configuration have to be determined with Table G of Annex G. However the general arrangement is given in Figure 5.5 together with the dimensions of the wheel print. Table 5.2 presents the values of the axle loads Q_{ik} for the three tandem systems.

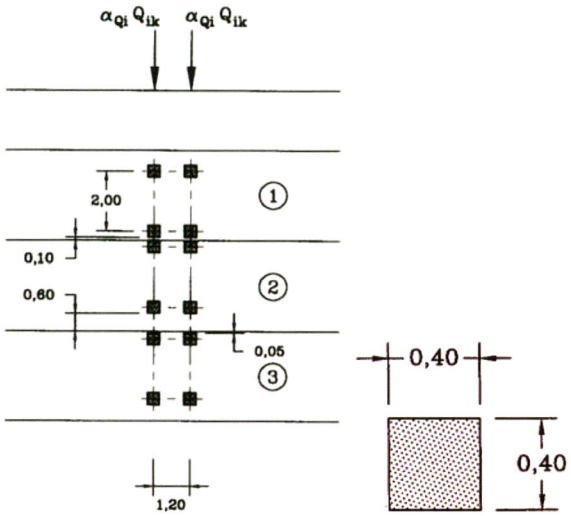

Figure 5.5 Tandem system arrangement and wheel print[3].

For expansion joints only the tandem systems TS apply. The uniformly distributed loads (UDL) which have to been considered when designing bridge structures are not relevant for expansion joints. The axle loads include dynamic amplification, except for the effects of resonance.

Table 5.2 Basic values for tandem systems.

Location	Tandem system	Axle loads Q_{ik}
Lane number 1	TS1	300 kN
Lane number 2	TS2	200 kN
Lane number 3	TS3	100 kN

As stated before the vertical loads are based on Load Model 1 from EN 1991-2. Some might have expected that the values of characteristic Load Model 2 should be applied, because this model uses a single axle load of 400 kN resulting in a higher local load introduction. But due to the larger wheel print of 0,35 * 0,60 m the contact pressure is almost equal to the contact pressure resulting from an axle load of 300 kN with a 0,40 * 0,40 m wheel print. However it should be noted that in case the shear resistance of a structural element is governing, Load Model 2 might result in a more adverse design situation than Load Model 1.

[3] Dimensions given in the figure are in meters.

5.3.3. Horizontal wheel loads

In the same way as for the vertical wheel loads, the horizontal loads are based on the values of characteristic Load Model 1 from EN 1991-2. The uniformly distributed load doesn't have to be considered here either.

Braking and acceleration force
It is assumed that the braking and acceleration forces act in the traffic direction only. For determining the values of these forces only tandem system 1 from Load Model 1 should be considered. The braking force shall be calculated with:

$Q_{lk} = b_k * \alpha_{Q1} * Q_{1k} = 120kN$

with $b_k = 0,4$, which is the characteristic value of the relationship between Q_{lk} and Q_{1k} for the deceleration effect, and α_{Q1} is 1,0.

Centrifugal forces
The centrifugal forces also are derived from Load Model 1:

$Q_V = \Sigma \alpha_{Qi} * Q_{ik}$

with α_{Qi} is 1,0 (for i = 1 to 3).

The centrifugal forces become: $Q_{tk} = 0,2 * Q_V$
For an axle on lane 1: $Q_{tk} = 60$ kN
For an axle on lane 2: $Q_{tk} = 40$ kN
For an axle on lane 3: $Q_{tk} = 20$ kN

In the design of an expansion joint these transverse forces have to be considered, because the joint can be located in a curve. Although its position remains perpendicular to the road stretch it can be subjected to centrifugal forces.
Here Annex G deviates from the conditions as depicted in paragraph 4.4.2 of EN 1991-2 by leaving the horizontal radius of the carriageway centreline out of the equation and using the factor 0,2, which is an upper bound value in Table 4.3 of EN 1991-2.

5.3.4. Fatigue loads

In Annex G two load models are described for the fatigue assessment of expansion joints. The first one, $FLM1_{EJ}$, is based on Fatigue Load Model 1 of EN 1991-2 and the second one, $FLM2_{EJ}$, which is a set of equivalent axles, is based on Fatigue Load Model 4. Whenever a check has to be made whether the fatigue life maybe considered as unlimited, $FLM1_{EJ}$ has to be used. The manufacturer may choose to use $FLM2_{EJ}$ as an alternative. This model makes use of a Palmgren-Miner summation in order to calculate the cumulative damage caused by traffic.
It should be noted that the load models in EN 1991-2 include dynamic load amplification appropriate for pavements of good quality and therefore dynamic amplification is also included in $FLM1_{EJ}$ and $FLM2_{EJ}$ for expansion joints.

Fatigue load Model 1 ($FLM1_{EJ}$)
For this model only one axle has to be considered. The vertical force resulting from this single axle shall be calculated with:

$Q_{1k,fat} = \Delta\varphi_{fat} * Q_{1k} * 0,7 = 273$ kN

with $\Delta\varphi_{fat} = 1,3$ and $Q_{1k} = 300$ kN.

In combination with a horizontal force of:

$Q_{1lk,fat} = 0,2 * \Delta\varphi_{fat,h} * Q_{1k} * 0,7 = 42$ kN in traffic direction

with $\Delta\varphi_{fat,h} = 1,0$.

The factors $\Delta\varphi_{fat}$ for vertical loads and $\Delta\varphi_{fat,h}$ for horizontal loads are additional dynamic amplification factors that represent unevenness and resonance at the expansion joint. However their values differ as can be seen from the above. The axle configuration and wheel print to apply are identical to that of static Load Model 1, as given in Figure 5.5.

Fatigue load Model 2 ($FLM2_{EJ}$)
When using this model, the number of vehicles can be selected from Table 4.5 of EN 1991-2 and the transverse distribution is given in Fig. 4.6 of EN 1991-2.
The interaction of vertical and horizontal axle load histograms is given in the table below. The loads mentioned in this table already include the dynamic amplification factors. The vertical axle load histogram is based on EN 1991-2, Table 4.7 for the "Medium Distance" traffic type. Different from the Eurocode, where for each type of lorry the equivalent load for each separate axle is given, Annex G uses an axle number rate. This rate in fact is a summation of the percentages of all lorry types, corresponding to a specific value of an axle load. Multiplying the axle number rate with the design lifetime and the number of vehicles on the slow lane, results in the number of cycles to be considered for an axle load.

Table 5.3 Vertical and horizontal loads for fatigue.

$Q_{1k,fat}$ Vertical axle load	$Q_{1lk,fat}$ Horizontal axle load in traffic direction	Axle number rate	Wheel print (length x width)
100 kN	-	1,1	300 x 300
120 kN	-	1,25	300 x 300
150 kN	20 kN	0,20	400 x 400
170 kN	24 kN	0,45	400 x 400
190 kN	28 kN	0,45	400 x 400

6. Analytical calculations

In this chapter the results of analytical calculations based on Annex G of the "Guideline for European Technical Approval of Expansion Joints for Road Bridges" (EOTA, 2006) will be presented and discussed. Whenever there is need for a reference to this document for simplicity it will be mentioned as Annex G. The traffic loads that have to be considered have been described in paragraph 5.3. The first paragraph of this chapter deals with the basic information and assumption necessary for the ultimate limit state verification, paragraph 6.2, and the fatigue verification, paragraph 6.3.

6.1. General

Subject of study for the analytical calculations is the WSG 320-type expansion joint, because this type has longer support bars than the other types present in bridge Heteren. Longer support bars have a larger influence on the structural behaviour. Essential for modelling of the construction and the calculations are the positions of the centre beams (joint gap) and the dimensions of the members.

6.1.1. Member properties

In Figure 6.1, the member properties as given in the original design calculations (Sollinger Hütte GmbH, 1999) are shown. The cross-sectional resistances mentioned in the figure are the elastic values.

Trägheitsmomente	[mm⁴]	J_y	30808962
bzgl. der Schwerachsen		J_z	3212355
Widerstandsmomente	[mm³]	W_y	335164
		W_z	71386
Schwerpunktkoordinaten	[mm]	y_S	45
bezogen auf den Nullpunkt		z_S	91,922
Fläche gesamt	[mm²]	A	6846
Fläche Steg	[mm²]	A_{St}	1950
Fläche Flansch	[mm²]	A_{Fl}	4500

Trägheitsmomente	[mm⁴]	J_y	11400000
bzgl. der Schwerachsen		J_z	3990000
Widerstandsmomente	[mm³]	W_y	190000
		W_z	75300
Fläche gesamt	[mm²]	A	5320

Figure 6.1 Left: Properties of the centre beams; Right: Properties of the support bars.

For calculation of the stress-ranges influencing the fatigue life time the elastic cross-section resistance is used. However for checking the structural safety of the members in the ultimate limit state usage of the plastic cross-section capacity might be allowed. Therefore the cross-section first has to be classified according to NEN-EN 1993-1-1. In Appendix paragraph III.1 it is shown that the cross-section requirements for global plastic analysis are met and the plastic capacities necessary for the various checks are determined. The results are given in the table below.

Table 6.1 Plastic resistance capacity of structural members.

	$N_{pl,Rd}$	$V_{pl,y,Rd}$	$V_{pl,z,Rd}$	$M_{pl,y,Rd}$	$M_{pl,z,Rd}$
Centre beam	$1{,}198 \cdot 10^3$ kN	399,67 kN	922,3 kN	169,34 kNm	41,68 kNm
Support bar	n.r.	369,75 kN	n.r.	83,71 kNm	n.r.

n.r.: not relevant for the analysis

6.1.2. Modelling

Starting point for modelling the expansion is the maximum opening position as declared by the manufacturer. From the construction drawing given in Appendix IV can be derived that the maximum gap opening is 80 mm. Since a wheel print of 400*400 mm has to be used and a centre beam is 90 mm wide, the most adverse situation occurs if two out of three centre beams are loaded by a wheel; see left part of Figure 6.2.
It should be noted that although here it is clear that the width of the expansion joint is smaller than the spacing between successive axles of a tandem system, see Figure 5.5, in case of larger modular expansion joints the structure might be loaded by successive axles of a vehicle.

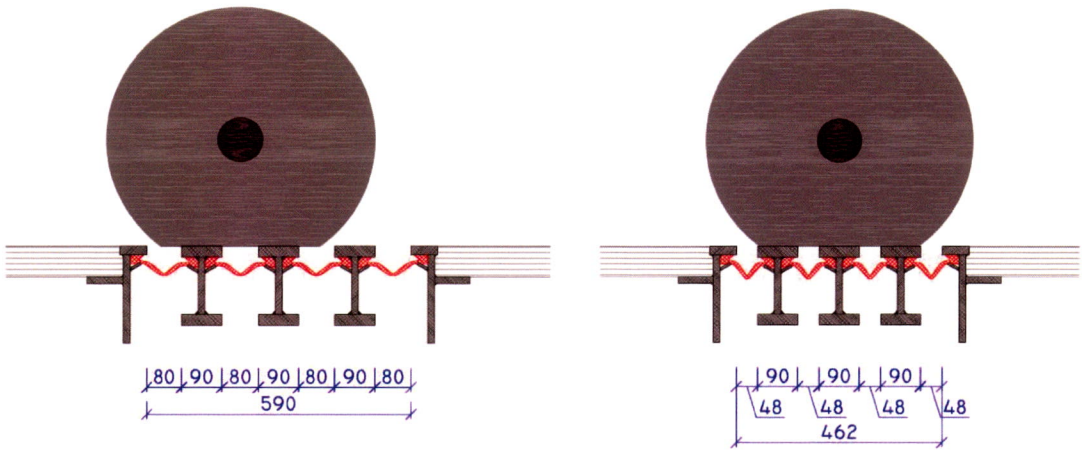

Figure 6.2 Left: Wheel on a joint at maximum opening; Right: Joint opened for 60%.

For fatigue lifetime calculations, a situation has to be considered where the joint is opened for 60% of the maximum declared opening position (ψ_{0d} = 0,6; paragraph 6.3). For the WSG-joint this results into an opening of 48 mm. This means that with a wheel length of 400 mm all three centre beams are loaded as can be seen in the right part of Figure 6.2. Also a 300*300 mm wheel print has to be considered for fatigue verification. This wheel print gives the most adverse loading when only two centre beams are loaded.

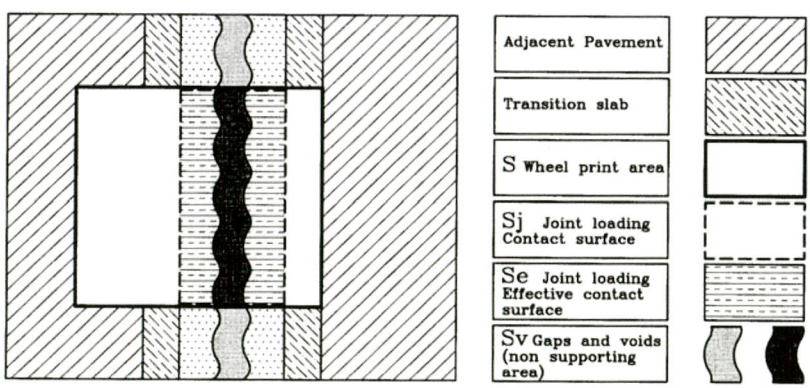

Figure 6.3 Definition of the surfaces influencing the contact pressure.

In general contact pressure resulting from one wheel can be calculated with the area definitions from the figure above and the following formula:

$\sigma_{contact} = Q_{wheel} / (S\text{-}Sv) = (Q_{axle} / 2) / (S\text{-}Sv)$
with S and S_v as defined in Figure 6.3.

For the WSG 320-type expansion joint the entire wheel print area S is carried by the centre beams for all design situations as explained previous. This means that the formula for the contact pressure can be simplified into:

$\sigma_{contact} = (Q_{axle} / 2) / S_e = (Q_{axle} / 2) / (N * W_{flange} * W_{wheel})$
N = number of centre beams carrying the wheel;
W_{flange} = the width of the top flange of a centre beam;
W_{wheel} = the width of the wheel print.

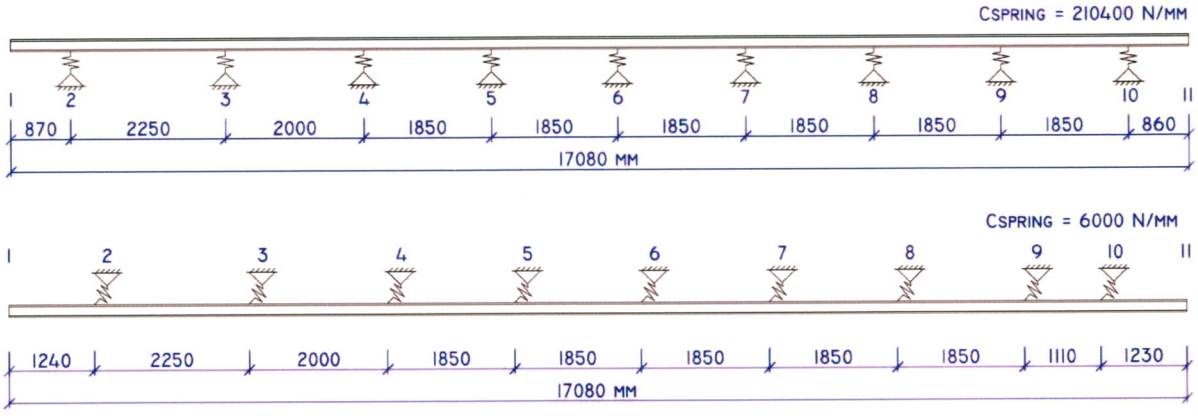

Figure 6.4 Static schemes for the vertical and horizontal support of a centre beam.

The centre beams are modelled as continues girders over multiple elastic supports, Figure 6.4. In vertical direction a centre beam is supported by elastic spring at the positions of the support bars. The horizontal elastic springs are placed at the location of the control springs of the joint, which are located 370 mm to the left or right of a support bar. Especially in comparison to the horizontal springs, the vertical springs have a rather high value, which results in a very rigid behaviour of the structure in vertical direction. This large vertical stiffness is a result of the stiffness of the support bar, the large stiffness of the support bar bearings and the large stiffness of the stainless steel plate between centre beam and support bar. The values for the spring stiffness in vertical and horizontal direction given in the figure were taken from the original design calculations.
Since the support scheme for a centre beam is too complex to calculate by hand due to the many springs, a simplistic calculation program is used to calculate the required internal beam forces for the centre beam. Verification of the support bar on the other hand does not require a computer program for calculation of internal forces. The support bar can be regarded as a simply supported beam.

6.2. Ultimate limit state calculation

Next step in the process is determining what loads should be considered for an ultimate limit state calculation. In paragraph 5.3 the relevant loads from Annex G were mentioned. With regard to the vertical loading two tandem systems have been applied, as bridge Heteren is a 2x2 motorway.
For determining the cross-section of the centre beam with the largest member forces influence lines are very useful. Unfortunately the simple calculation program used does not contain a moving load function. Therefore a different approach was used. The resultant force of the two tandem systems for the vertical loading were positioned either at the field middle between two elastic supports or at the location of the elastic support. One can see it as a semi-moving load with a lot of load cases, Figure 6.5. The figure actually shows the tandem systems at the most adverse loading situation.

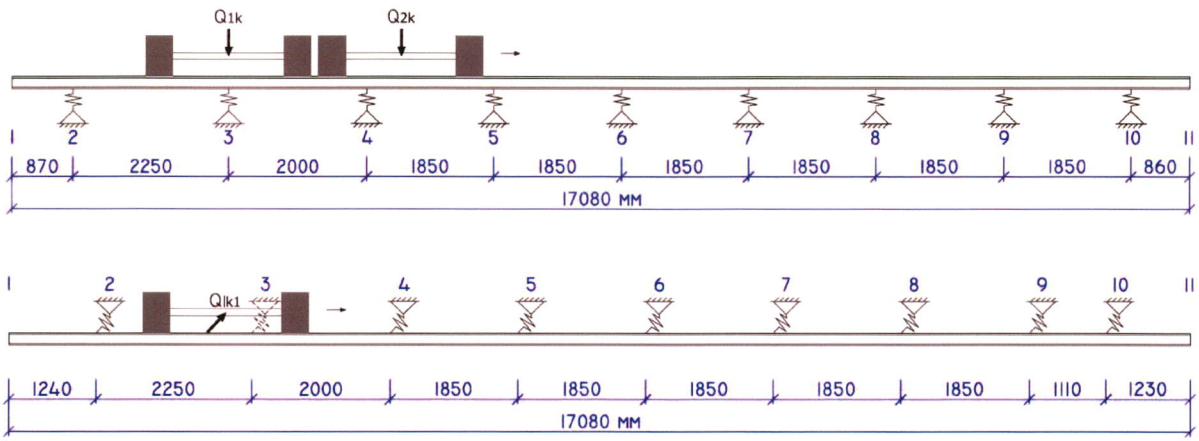

Figure 6.5 Top: Moving load for vertical axle forces; Bottom: Moving load for the braking force.

The axle forces were not inserted in the model as point loads, but as distributed line loads since the contact pressure of a wheel print has to be considered, see Appendix paragraph III.2. These distributed line loads are obtained by leaving the width of a centre beam out of the formula for the contact pressure. To give an indication, values of the distributed loads are given in the table below for the situation of maximum gap opening.

Table 6.2 Values for the distributed line loads applied for ψ_{0d} = 1,00.

Load no. i	Vertical q_{ik}	Braking q_{lki}	Centrifugal q_{tki}
1	187,5 kN/m	75,0 kN/m	37,5 kN/m
2	125,0 kN/m	-	25,0 kN/m

With this different approach the largest field moment and hogging moment could be obtained. The highest value for the field moment and hogging moment are found respectively in the part between node 3 and 4, and at the second support (node 3). The results found for the member forces are given in Table 6.3.
A similar table could be made for the situation with reduced opening of the joint (ψ_{0d} = 0,60) simply by multiplying the results with a factor 2/3, because three instead of two centre beams support the wheel. Here the choice has been made to implement this factor directly in the calculation of the design values. See Appendix paragraph III.2.1.

Table 6.3 Results for member forces at maximum joint opening (ψ_{0d} = 1,00).

	Maximum field moment	Maximum hogging moment
Moment - dead weight	0,13 kNm	-0,21 kNm
Moment - vertical TS load	23,10 kNm	-30,09 kNm
Moment - horizontal TS load	4,89 kNm	-2,47 kNm
Shear force - dead weight	0 kN	-0,61 kN
Shear force - vertical TS load	0 kN	-55,04 kN
Shear force - horizontal TS load	8,08 kN	-15,36 kN
Normal force	11,2 kN	15 kN

For verification of the static strength at the ultimate limit state the formula given hereafter, has to be used for the various design combinations. In the equation, the sign "+" means "In combination with".

$\mathbf{C_{ULS}} = \gamma_{Gi}G_k$ "+" $\gamma_F F_{ik}$ "+" $\psi_{0T}\gamma_{Q1}$ [Q_{1k} "+" ($\psi_{0lk} Q_{lk1}$ "+" $\psi_{0tk} Q_{tk1}$) "+" Q_{2k} "+" ($\psi_{0tk} Q_{tk2}$)"+" Q_{3k} "+" ($\psi_{0tk} Q_{tk3}$)] "+" $\gamma_{dE}\psi_{0d}d_{Ek}$
d_{Ek}: Maximum opening position of the joint declared by the manufacturer;
F_{ik}: Characteristic internal force.

In this formula the partial factors to be applied are taken from Table G4 of Annex G and have the following values: γ_{Gi} = 1,35; γ_{Qi} = 1,35; γ_{dE} = 1,00. The combination factors to be used are given in the table below.

Table 6.4 Combination factors ψ_0.

C_{ULS}	Design situation	ψ_{0T}	ψ_{0d}	ψ_{0lk}	ψ_{0tk}
1	Reduced opening position with maximum traffic loads, flowing traffic with centrifugal effects	1,00	0,60	0,00	0,50
2	Maximum opening position with reduced traffic loads, braking traffic with centrifugal effects	0,70	1,00	0,50	0,50

ψ_{0T}: combination factor for traffic loads;
ψ_{0d}: combination factor for the opening position;
ψ_{0lk}: combination factor for traffic loads in the traffic direction;
ψ_{0tk}: combination factor for traffic loads perpendicular to the traffic direction.

From this table it can be seen that two design combinations can be governing for the verification of the static strength. With use of the combination factors, the results for the member forces at maximum opening position and the combination formula, the design values for the location of the maximum field and hogging moment and for the forces acting on the support bar are calculated. See Appendix paragraph III.2.1. The results of these calculations are presented in the Tables 6.5 till 6.7.

Table 6.5 Design values maximum field moment

	N_{Ed}	$V_{Ed,\ vertical}$	$V_{Ed,\ horizontal}$	$M_{Ed,\ vertical}$	$M_{Ed,\ horizontal}$
C_{ULS-1}	5,04 kN	0 kN	0 kN	20,97 kNm	0 kNm
C_{ULS-2}	5,29 kN	0 kN	3,82 kN	22,01 kNm	2,31 kNm

Table 6.6 Design values maximum hogging moment

	N_{Ed}	$V_{Ed,\ vertical}$	$V_{Ed,\ horizontal}$	$M_{Ed,\ vertical}$	$M_{Ed,\ horizontal}$
C_{ULS-1}	6,75 kN	50,36 kN	0 kN	-27,36 kNm	0 kNm
C_{ULS-2}	7,09 kN	52,84 kN	7,26 kN	-28,77 kNm	-1,17 kNm

Table 6.7 Design values maximum forces from centre beam on support bar

	$F_{vertical}$	$F_{horizontal}$	$M_{t,d}$
C_{ULS-1}	112,50 kN	0 kN	0 kNm
C_{ULS-2}	118,04 kN	15,46 kN	2,94 kNm

The design values found for C_{ULS-1} represent a less adverse design situation for the expansion joint than the values found for C_{ULS-2}. Therefore only the latter have been checked according to Eurocode NEN-EN 1993-1-1.
Verification of the static strength, Appendix paragraphs III.2.2 and III.2.3, shows that the most adversely loaded centre beam, support bar and support bearing of the support bar have sufficient capacity to withstand the traffic loads given in Annex G. The results of the unity checks performed are also presented in the table below. Based on the values for these checks it is expected that the support bar will be the governing structural element for the fatigue life of the joint construction.

Table 6.8 Results unity checks for structural members at ULS.

Member	Verification	Value unity check
Centre beam	Maximum field moment	0.072
	Maximum hogging moment	0.057
Support bar	Maximum bending moment	0.45
	Support bearing capacity	0.42

6.3. Fatigue calculation

In the original design calculation based on the desired design lifetime a check was made whether or not the construction would fail due to fatigue within the design life, see Appendix V. Here a different approach has been used. By making use of Fatigue load Model 2 ($FLM2_{EJ}$) of Annex G, the fatigue damage resulting from different stress ranges are determined for four important sections of the construction and with it the fatigue lifetime was calculated.

For verification of the fatigue life a choice has to be made between 2 different design philosophies. These are the damage tolerant method and the safe life method. Here the damage tolerant method with the assumption that the consequences of failure are high is applied. This means that for the fatigue strength a value of γ_{Mf} = 1,15 is used, see Table 6.9. The basis of damage tolerant design is that periodic inspection and maintenance for detecting and repairing fatigue damage is performed throughout the design lifetime of the structure, which is the case for this expansion joint as it easily accessible for inspection.

Table 6.9 Partial factors γ_{Mf} for fatigue strength.

Assessment method	Consequence of failure	
	Low consequence	High consequence
Damage tolerant	1,00	1,15
Safe life	1,15	1,35

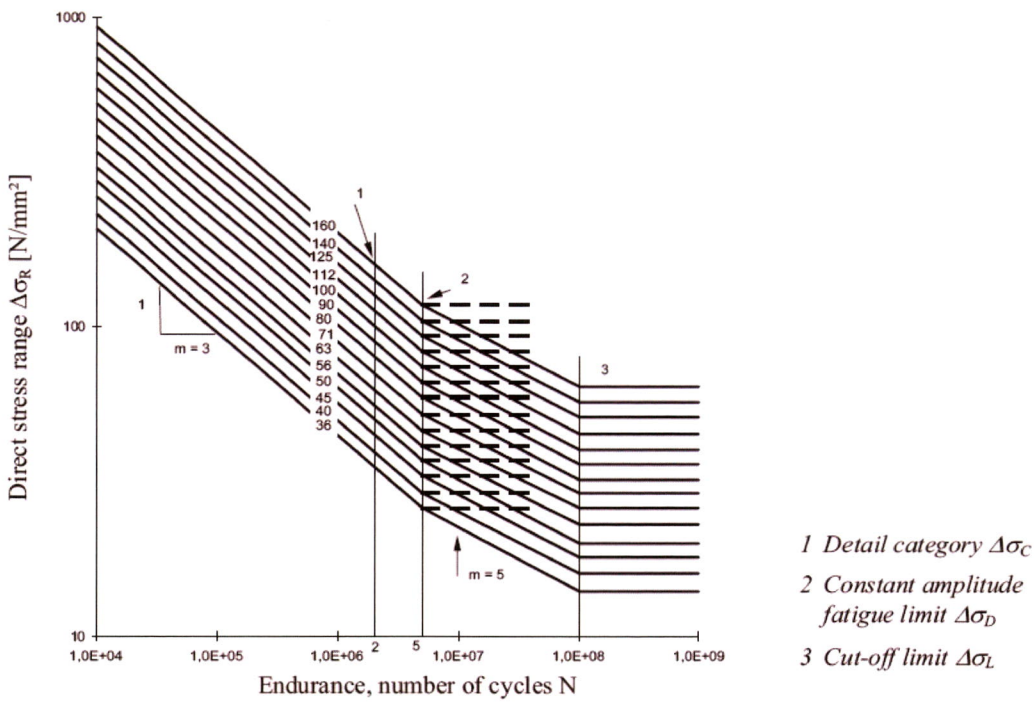

Figure 6.6 Fatigue strength curves for stress ranges.

Four different cross-sections of the expansion joint members are considered for the fatigue calculation. These are a field location of a centre beam, the support of the centre beam on the support bar, the centre beam at the location of the prestressed bolted connection, as shown in Figure 6.7, and the field location of a support bar. For fatigue assessment of these locations or element first a specific fatigue property, the so-called detail category, has to be determined.
The detail category is a numerical designation used in order to indicate which fatigue strength curve, Figure 6.6, is applicable for the fatigue assessment. The detail category corresponds to the stress range at $2{,}0 \cdot 10^6$ cycles and with the use of relationships following from the fatigue strength curve the stress limits in the curve can be calculated (Romeijn, 2005). The results for these stress limits are presented in Table 6.10. Also the construction details on basis of which the detail categories are determined, are mentioned in this table.

Table 6.10 Fatigue properties and stress limits of structural members according to NEN-EN 1993-1-9.

	Construction detail	Detail category	$\Delta\sigma_C$ [N/mm²]	$\Delta\sigma_D$ [N/mm²]	$\Delta\sigma_L$ [N/mm²]
Centre beam	No 1, table 8.2	125	108,70	80,09	43,99
Centre beam at the location of prestressed bolted connection	No 10, table 8.1	90	78,26	57,66	31,67
Support bar	No 2, table 8.1	160	139,13	102,51	56,31

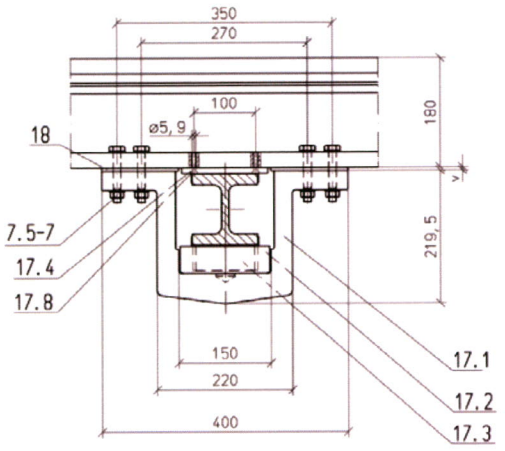

Figure 6.7 Detail drawing of the prestressed bolted connection.

The structure is modelled in the same way as was done for the ULS-calculation, Figure 6.8. The difference is that for both vertical and horizontal loads only one tandem system has to be applied. From the ULS-calculation data for the horizontal braking force it became clear that the most adverse loading due to one tandem system occurs when the resultant of the load is positioned at 3,120 meter from the left end of the centre beam. Therefore only one load case has to be considered.
Identical to the ultimate limit state calculation the axle forces were not inserted in the model as point loads, but as distributed line loads since the contact pressure of a wheel print has to be considered, see Appendix paragraph III.3. The way how to calculate these distributed line loads and how many centre beams are loaded, has been explained earlier in this chapter in paragraph 6.1.2.

The combination for checking the structure in the fatigue limit state is:
$\mathbf{C_{FAT}}$= F_{ik} "+" [$Q_{1k,fat}$ "+" $Q_{lk1,fat}$] "+" $\psi_{0d}d_{Ek}$
F_{ik}: Characteristic internal force;
d_{Ek}: the maximum declared opening position of the joint;
ψ_{0d} = 0,6. This is a so-called combination factor.
Also in this formula the sign "+" means "In combination with".

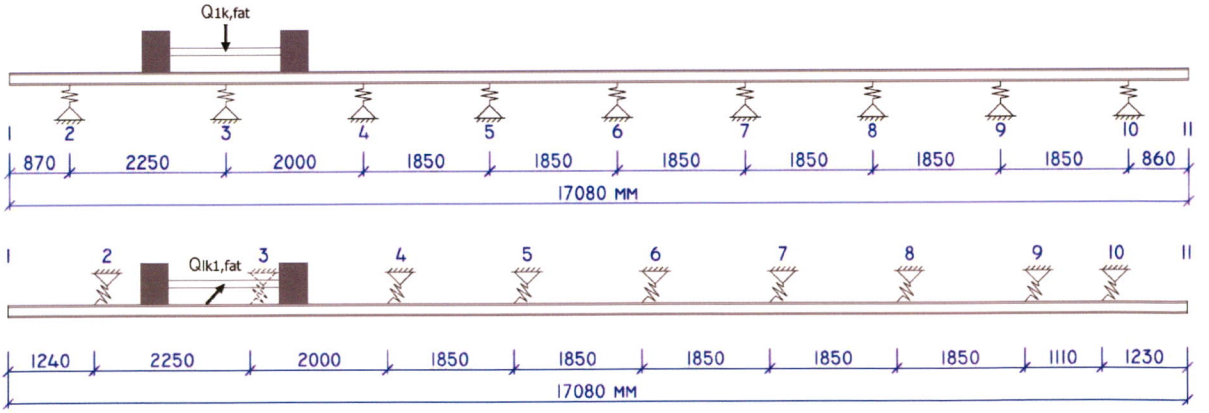

Figure 6.8 Vertical and horizontal fatigue loads at the most adverse position.

With this information the vertical and horizontal moments corresponding to the different combinations of axle loads have been determined. For the support bar and the centre beam at the location of the bolted connection additional calculations were made in order to obtained the necessary results. These calculations are presented in Appendix paragraph III.3.1 and III.3.2.
According to Ramberger (2002) the stress ranges can be determined with the following formula:

$$\Delta\sigma_{k,max,dyn} = \Delta M_{v,k,dyn} / W_{vertical} + \Delta M_{h,k,dyn} / W_{horizontal}$$

The values of the occurring moments and the results for the stress ranges are given in the Table 6.11 till 6.14. With the use of the fatigue strength curve and the stress ranges the corresponding number of cycles N are calculated.

For the fatigue lifetime calculation only one more parameter had to be determined. That is the number of heavy vehicles expected per year per slow lane. Here traffic category 1 (Table 4.5, NEN-EN 1991-2), which gives $N_{obs} = 2{,}0 \cdot 10^6$ vehicles per year, was chosen. This is identical to the number of vehicles used in the original design calculation. See Appendix V. Multiplying this number with the axle number rate and the design lifetime of 30 years gives the corresponding number of axle types, represented in Table 6.11 till 6.14 as n. When the action n/N and a Palmgren-Miner summation are applied, the cumulative damage values D are known for the four cross-sections of the expansion joint members.

It should be noted that in the column n/N of all four tables, the value 0,000 appears if the number of cycles N becomes larger than $1{,}0 \cdot 10^8$. It means that the stress range is lower than the cut-off limit $\Delta\sigma_L$, see Figure 6.6, and therefore does not contribute to the fatigue damage.

Table 6.11 Cumulative damage calculation for the centre beam at field location.

Vertical axle load [kN]	Horizontal axle load [kN]	Axle number rate	n	Vertical moment [kNm]	Δσ-vertical [N/mm2]	Horizontal moment [kNm]	Δσ-horizontal [N/mm2]	Δσ-total [N/mm2]	N	n/N
100	-	1,1	6,60E+07	8,17	24,38	0,00	0,00	24,38	1,91E+09	0,000
120	-	1,25	7,50E+07	9,80	29,25	0,00	0,00	29,25	7,69E+08	0,000
150	20	0,2	1,20E+07	7,94	23,69	1,20	16,81	40,50	1,51E+08	0,000
170	24	0,45	2,70E+07	9,00	26,85	1,44	20,17	47,02	7,17E+07	0,377
190	28	0,45	2,70E+07	10,06	30,01	1,68	23,53	53,54	3,74E+07	0,721
									D = Σn/N =	1,098

Table 6.12 Cumulative damage calculation at the support of the centre beam on the support bar.

Vertical axle load [kN]	Horizontal axle load [kN]	Axle number rate	n	Vertical moment [kNm]	Δσ-vertical [N/mm2]	Horizontal moment [kNm]	Δσ-horizontal [N/mm2]	Δσ-total [N/mm2]	N	n/N
100	-	1,1	6,60E+07	-8,92	26,61	0,00	0,00	26,61	1,23E+09	0,000
120	-	1,25	7,50E+07	-10,70	31,94	0,00	0,00	31,94	4,96E+08	0,000
150	20	0,2	1,20E+07	-8,87	26,46	-0,27	3,78	30,25	6,51E+08	0,000
170	24	0,45	2,70E+07	-10,05	29,99	-0,32	4,54	34,53	3,35E+08	0,000
190	28	0,45	2,70E+07	-11,24	33,52	-0,38	5,30	38,82	1,87E+08	0,000
									D = Σn/N =	0,000

Table 6.13 Cumulative damage calculation for the centre beam at the bolted connection.

Vertical axle load [kN]	Horizontal axle load [kN]	Axle number rate	n	Vertical moment [kNm]	Δσ-vertical [N/mm2]	Horizontal moment [kNm]	Δσ-horizontal [N/mm2]	Δσ-total [N/mm2]	N	n/N
100	-	1,1	6,60E+07	-6,50	19,39	0,00	0,00	19,39	1,16E+09	0,000
120	-	1,25	7,50E+07	-7,80	23,27	0,00	0,00	23,27	4,67E+08	0,000
150	20	0,2	1,20E+07	-6,46	19,27	-0,54	7,49	26,77	2,32E+08	0,000
170	24	0,45	2,70E+07	-7,32	21,84	-0,64	8,99	30,84	1,14E+08	0,000
190	28	0,45	2,70E+07	-8,18	24,41	-0,75	10,49	34,91	6,15E+07	0,439
									D = Σn/N =	0,439

Table 6.14 Cumulative damage calculation for the support bar.

Vertical axle load [kN]	Horizontal axle load [kN]	Axle number rate	n	Vertical moment [kNm]	Δσ-vertical [N/mm2]	N	n/N
100	-	1,1	6,60E+07	9,01	47,44	2,36E+08	0,000
120	-	1,25	7,50E+07	10,82	56,93	9,47E+07	0,792
150	20	0,2	1,20E+07	12,67	66,68	4,29E+07	0,280
170	24	0,45	2,70E+07	14,36	75,58	2,30E+07	1,176
190	28	0,45	2,70E+07	16,05	84,47	1,32E+07	2,051
						D = Σn/N =	4,299

The design life of a WSG-type girder grid joint is assumed to be 30 years, Appendix V. The fatigue lifetime of a structural element can be calculated easily by dividing the design lifetime of 30 years by the cumulative damage value D. For example, failure of the centre beam at a field location will occur after a fatigue lifetime of 30 / 1,098 = 27 years. The results found for the fatigue lifetime of the four cross-sections of the expansion joint members are given in the table below.

Table 6.15

	Fatigue lifetime
Centre beam at field location	27 years
Support of centre beam on support bar	sufficient
Centre beam at the location of the bolted connection	sufficient
Support bar	7 years

Reflection on results

The choice for the assessment method and the appropriate safety factor has a large influence on fatigue life. How the lifetime is influenced becomes very clear when the value for the partial safety factor is altered. The results are given in Table 6.16. The value 1,25 for the safety factor was used by Sollinger Hütte in their calculations, as can be seen in Appendix V.

Table 6.16 Influence of the partial factor for strength on the fatigue life of the support bar.

Value for γ_{Mf}	Cumulative damage value D	Lifetime
γ_{Mf} = 1,00	1,743	17 years
γ_{Mf} = 1,15	4,299	7 years
γ_{Mf} = 1,25	6,523	5 years

Another example of the influence of the design choices made is illustrated by the following. Recently the members of Working Group 01.07/02 "Expansion joints" who are establishing ETAG No 32 (EOTA, 2006), have decided that the number of heavy vehicles per year per slow lane traffic used in the fatigue verification will be lowered from $2,0 \cdot 10^6$ to $5,0 \cdot 10^5$ vehicles. Of course this also implies that for the fatigue design of the adjacent bridge structure the number of trucks reduces.
Alteration of the number of vehicles in the fatigue calculation, with γ_{Mf} = 1,15, shows that the fatigue lifetime of the support bar improves very much. Instead of a fatigue lifetime of 7 years, now a lifetime of 28 years is achieved. This lies very close to the original design lifetime of 30 years.

7. Finite element modelling

Finite element modelling always consists of three phases: pre-process, analysis and post-process. The success of the analysis and accurate results, fully depend on the choices made in the pre-processing phase. Goal of this chapter is therefore to clarify these choices. In the second paragraph the finite element model of the WSG 320 modular expansion joint of Bridge Heteren is described. The last paragraph shows the options chosen for the analysis.

7.1. Why FEM?

One could wonder why to use a complex, time-consuming computer program when it already is possible to gain quite an idea about the member forces in a structure by means of an analytical calculation. As this also applies to the type of expansion joints under consideration, an explanation for this choice will be given.
The usage of a finite element analysis program gives better opportunities to model the three dimensional behaviour of the structure under the different load combinations. Aspects as differences in member stiffness, multiple degrees of freedom, time-dependent loading and natural frequencies now can be considered much better.
Beside these theoretical arguments there is also a more practical application that adds value to the use of a finite element program. As the perfect situation does not occur due to uncertainties during design phase and inaccuracies in execution, reality never corresponds with the design drawings directly. Usage of analysis software allows for easy change of variables, such as boundary conditions or spring stifnesses for example, and comparison of their influence, as is shown in paragraph 8.3.2.

MIDAS/Civil
The finite element analysis program used is MIDAS/Civil. This analysis program tries to distinguish itself from other numerical analysis programs by offering an integrated civil engineering system for designing bridges and civil structures in general. It contains tools for construction stage analysis for prestressed/post-tensioned concrete, suspension, cable-stayed and conventional bridges and heat of hydration analysis.

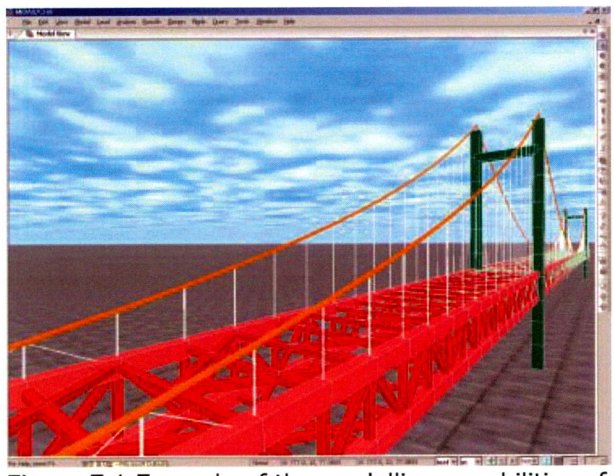

Figure 7.1 Example of the modelling capabilities of MIDAS/Civil.[4]

[4] The figure is taken from the MIDAS/Civil 'Getting started'-manual, MIDAS Information Technology Co., Ltd. (2006).

7.2. The reference model

This paragraph has been divided in four subparagraphs, which are devoted to different aspects or subparts of modelling the WSG 320 modular expansion joint.

7.2.1. Conceptualisation

For the analytical calculation the complete expansion joint with its total length of 17 meters was modelled, see paragraph 6.1.2. While processing the output for relevant results it could be seen that the influence of the axle loads is limited to a few fields. This is also shown in the figure below.

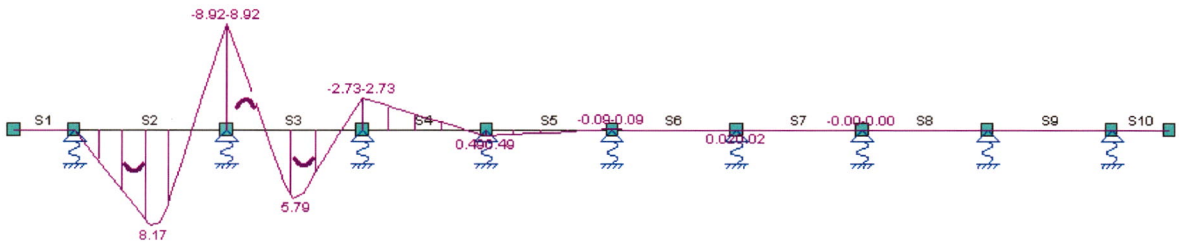

Figure 7.2 Bending moment line as a result of a vertical fatigue axle load shows the influence area.

Based on this information it was decided not to consider the complete expansion joint for the finite element model, but only the part influenced by the load. This implied the centre beams over a length of 8820 mm and five support bars, see Figure 7.3. The gaps between the centre beams are 48 mm. Next step in the process was defining a mesh. A mesh divides a structure into a number of elements and requires nodes in order to connect these elements. Some first sketches for a mesh are shown in Appendix VI. The sketches provided a quick overview of convenient locations of nodes and dimensions of elements. Beam elements were applied as they are easy to generate and the desired results can be extracted quickly from the analysis output.

However, at a later stage it became clear that in order to be able to model the dynamic loading more accurate with the usage of time forcing functions for a time history analysis, which will be discussed later in this chapter, more nodes were required for the top flanges of the centre beams. Therefore the choice was made to shift from beam elements to plate elements for the centre beams of the expansion joint. As the width of a flange is 90 mm, the height of a web is 130 mm and the support bars are located at centre-to-centre distances that allow for division by 50, a mesh was generated with elements dimension of 45 x 50 mm for the flanges and 42,5 x 50 mm for the webs. Only for the last part of the cantilever, plate elements with a length of 70 mm were used. The final version of the finite element model is shown in the figure below, where traffic drives in the X-direction.

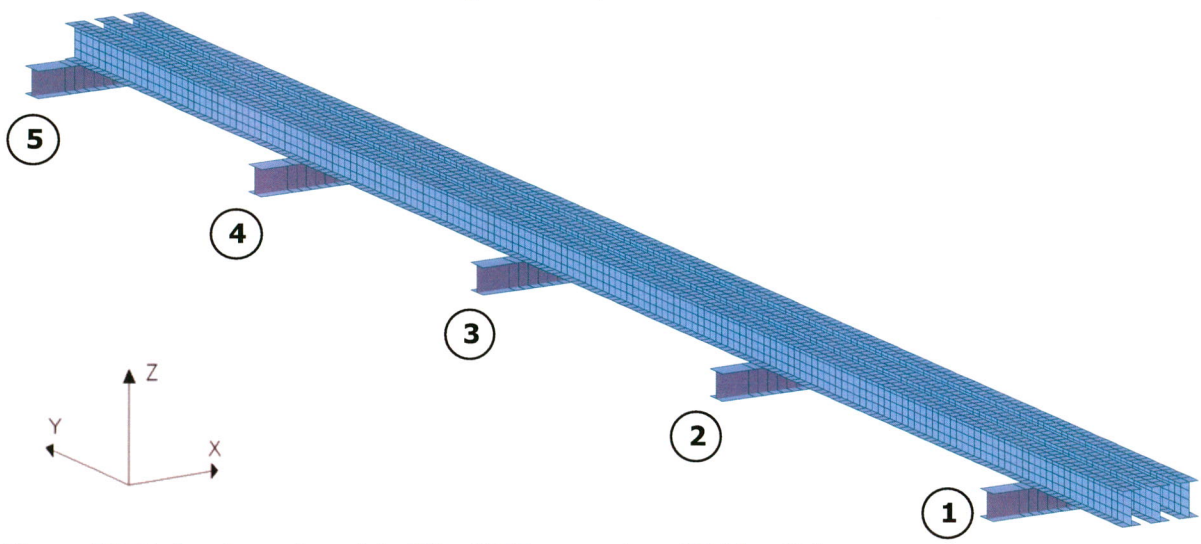

Figure 7.3 Finite element model of the WSG expansion of Bridge Heteren.

The support bars in Figure 7.3 have been given numbers for convenience, as these numbers will be mentioned frequently in the next chapter when discussing the results. Related to this, some definitions used are important too. If the description "end field" is mentioned the span between the first and second support bars are meant. The spans between the other support bars are denoted as "middle fields", e.g. the first middle field is the span between support bar two and three.

7.2.2. Composition

The finite element model does not simply exist out of beam and plate elements. Connections between these structure elements and the interaction with the appending structures also needs to be modelled. The options considered will be presented in the following part.

Structures
As stated before, the model consists of beam and plate elements. Before these elements could be made some options had to be chosen, which will be described hereafter. The sign and node designation for the beam and plate elements is given in Figure 7.4.

The beam elements have a material and cross-section property. The material property can be taken either from a database or defined by the user. The support bars are made of S355 construction steel and thus the properties were already available in the program. Also for the cross-section applies that a profile can be selected from the database or entered manually. As the support bars are of the type HEM-100 this standard section has been selected from the database.
The plate elements have a material and a thickness property, which is just the thickness of the plate. As the centre beams are made of the same steel as the support bars the same material property was selected. As described before the plates have a rectangular shape with almost equal in-plane dimensions. This gives length-to-width-ratios close to an aspect ratio of 1:1, which yields an optimum solution. Furthermore the option "thick" plate element has been selected, which implies that the program applies the Mindlin-Reissner plate theory, because the thickness of the flanges is quite large in respect to the width.

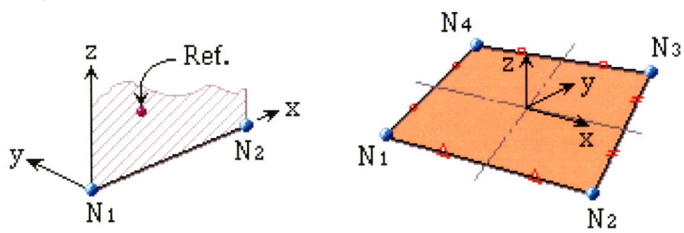

Figure 7.4 A beam and plate element with node designation (taken from the MIDAS/Civil program).

Boundaries
Two categories of boundary conditions can be distinguished. These are nodal boundary conditions and element boundary conditions. Three types (i.e. constraint for degree of freedom, elastic boundary element, elastic link element) belonging to the first category and one (i.e. rigid link) belonging to the second have been applied in the model. All four are shown in Figure 7.5 and summarized below with a short description of its function.

- Constraint for degree of freedom. This condition is used at both ends of the support bars. As mentioned in paragraph 3.1, a support bar is simply supported. Therefore, at one end all translations and at the other end the translations in Y- and Z-direction are obstructed;
- Elastic link elements have been used to model the control springs located in between the centre beams. The elastic links are placed at a distance of 350 mm from the support bar instead of 370 mm as was done for the analytical calculation, because the mesh of the centre beams in longitudinal direction is divided in pieces of 50 mm.
  In the reference model the elements have been given a value for the elastic stiffness in the X-direction only. This is in fact the dynamic stiffness in longitudinal direction of the control springs as taken from RW Sollinger Hütte GmbH (2007), which amounts 26090 N/mm.

In the same document it is stated that the stiffness of this rubber block in vertical direction is not known from tests results, but at least can be taken equal to the dynamic stiffness in longitudinal direction, because the static vertical stiffness is about 3,7 times higher than the horizontal stiffness as shown by Freundt (2007). The influence of this vertical stiffness has been studied in a parameter study and results will be discussed in the next chapter;

- Elastic Boundary element. In the program this condition is known as a point spring support and is applied to model the control spring that connects the centre beams to the edge beam. For these elements the same values for the stiffness as for the elastic link elements apply;

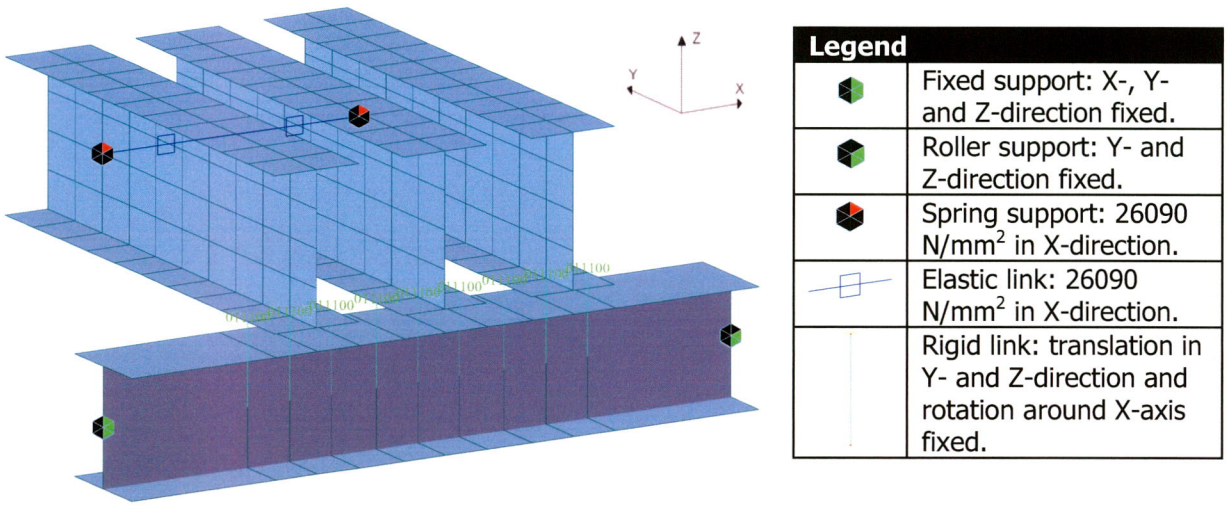

Figure 7.5 Cut-out of the model with all applied types of boundaries.

- Rigid links function as tying elements. They constrain geometric, relative movements of the structure. The centre beams are able to slide over the support bars in X-direction, while the support bars do not displace in this direction, but the beams do govern the other movements of the support bar. This means that the nodes of the bottom flanges are the master nodes and the support bar nodes are slave nodes, which are subordinated to the master nodes. At first all movements, except for the translation in X-direction, were constrained with one rigid link between a centre beam and a support bar, but testing then showed that the centre beam would start to rotate around the node in the flange. To tackle this problem six more nodes were added to the support bar and each centre beam got two additional tying elements. Now each link has the properties of a rigid plane connection in the Y-Z-plane, which means that translations in the Y- and Z-direction, and rotation around the X-axis are prevented.

In the description of the WSG-type joint in paragraph 3.1, has also been mentioned that movement of the centre beams over the support bar by means of stainless steel sliding plates only occurs when the horizontal traffic force is large enough to overcome the friction force. An attempt was made to model the friction force by means of general link elements at the same locations as the rigid links. General link elements can be used in MIDAS/Civil to model various elements such as dampers, base isolators, compression-only element, tension-only element, plastic hinges, soil springs, etc. The general springs were applied as hysteretic system type non-linear springs. However, testing of the model with these elements did not provide results in line with practical experience. Due to time limitations these non-linear springs could not be further investigated and therefore the general links are omitted. Instead the extreme situation where all movements of the centre beams relative to the support bars at the connection are obstructed will be investigated during the parameter study in order to study the relevance of friction elements in a model of WSG-type joints.

7.2.3. Static and dynamic loading

Self-weight
By selecting the material properties the beam and plate elements automatically get a mass density. This made applying the dead load due to self-weight very easy. The only variable that had to be specified was the direction in which the gravity force works on the structure. With the definition shown in Figure 7.6 and a factor of –1 for the Z-direction all necessary data is known.

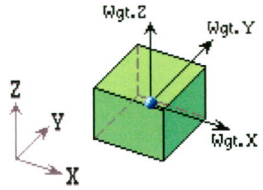

Figure 7.6 Visualisation of self-weight (taken from the MIDAS/Civil program).

Plane loads
In order to be able to calculate dynamic factors for the structural members, the internal forces due to the axle load for the static situation had to be determined. In fact this is the same situation as was studied for the fatigue analysis of the analytical calculations. Therefore the information described in paragraph 6.1.2 and the loads from paragraph 5.3.4 could be used.

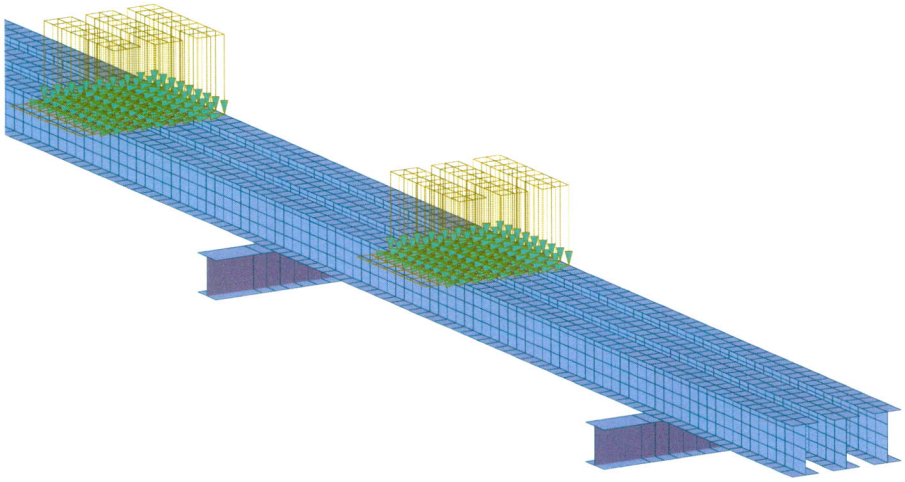

Figure 7.7 Combination of vertical and horizontal loading

The fatigue loads of Annex G (EOTA, 2006) already contain dynamic factors. Because we want to determine these factors for this particular structure, factors have to be extracted from the loads. Therefore the vertical and horizontal axle load are divided by respectively $\Delta\varphi_{fat}$=1,3 and $\Delta\varphi_{fat,h}$=1,0. With the formula for the contact pressure presented in paragraph 6.1.2, the values for the plane load-function can be determined. The results are presented in Table 7.1.
Again the wheels load the end and first middle field, as the resultant force of the axle load lies above the second support bar, see Figure 7.7. It should be emphasised that the real division of the traffic lanes over the width of the bridge has not been considered, but that the axle load is placed at the most adverse location. It is important to keep this in mind, when looking at the results.

Table 7.1 Vertical and horizontal loads used in the numerical analysis.

Vertical axle load	Horizontal axle load	Equivalent load combination	Beams loaded	Vertical contact pressure	Horizontal contact pressure
100 kN	-	76.9 kN	2	0.71 N/mm^2	-
120 kN	-	92.3 kN	2	0.85 N/mm^2	-
150 kN	20 kN	115.4 + 20 kN	3	0.53 N/mm^2	0.093 N/mm^2
170 kN	24 kN	130.8 + 24 kN	3	0.61 N/mm^2	0.111 N/mm^2
190 kN	28 kN	146.2 + 28 kN	3	0.68 N/mm^2	0.123 N/mm^2

Loads for the time history analysis

In order to generate a dynamic loading in MIDAS/Civil data concerning time history functions and dynamic loads has to be entered as part of a time history analysis. This type of analysis is described in paragraph 7.3.2. It is assumed that trucks pass the modular expansion joint with a velocity of 90 km/h, which is 25 m/s. This means that each centre beam is loaded for a time period of:

T= (90+300) $\cdot 10^{-3}$ m / 25 m/s = 0,0156 seconds in case of a 300 x 300 mm^2 wheel print;

T= (90+400) $\cdot 10^{-3}$ m / 25 m/s = 0,0196 seconds in case of a 400 x 400 mm^2 wheel print.

In literature different formulations can be found modelling the load on a centre beam as a function of time that have a triangular or sinusoidal shape. In his research on the subject of dynamics of expansion joints Steenbergen (2003) presents the following formula for the distribution of a load on a centre beam:

$$F(t) = \frac{F_{max}}{2} \cdot (1 - \cos\frac{2\pi \cdot t}{T})$$

with F_{max} according to Table 7.2

and T the duration of loading for a node, which is the wheel length divided by the velocity.

Table 7.2 The five load combinations with maximum values for each loaded node.

L.C No.	Vertical axle load	Horizontal axle load	Wheel print	Number of nodes	Vertical load per node F_{max}	Horizontal load per node F_{max}
1	76.9 kN	-	300 x 300	7	2747 N	-
2	92.3 kN	-	300 x 300	7	3297 N	-
3	115.4 kN	20 kN	400 x 400	9	2137 N	370 N
4	130.8 kN	24 kN	400 x 400	9	2422 N	444 N
5	146.2 kN	28 kN	400 x 400	9	2707 N	519 N

The last step necessary with regard to defining the time functions are the time steps for applying the load. A time increment of 0,4 ms has been chosen, which means that for load combination number 1 and 2 the load period is divided in 39 steps and for numbers 3 to 5 in 49 steps. An example of the appearance of a time history function is shown in Figure 7.8.

In the table above the number of nodes that are considered in the longitudinal direction of the centre beam have been mentioned. The front of a wheel arrives at all nodes of a row at the same moment. Since each flange of the three centre beams is divided in three nodes in traffic-direction, nine rows can be distinguished in total. For each row the arrival time was calculated, with the first row of the first centre beam as starting point (t = 0 s). Then all nodes on a row were given the same dynamic nodal load, consisting of the corresponding arrival time and the time function.

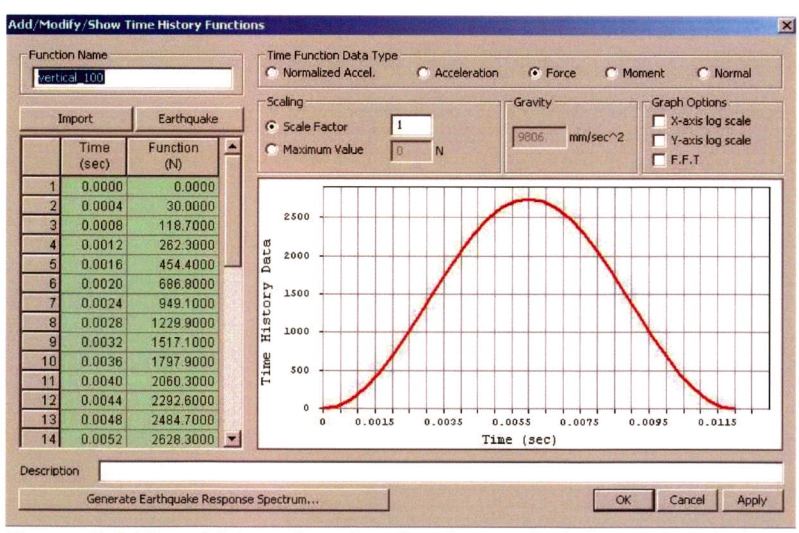

Figure 7.8 Time history function for the vertical dynamic axle load of 76,9 kN.

The formulation as derived by Steenbergen, as stated before, applies to each centre beam, because he modelled the centre beams as line elements. The difference is that the model used in this research is more refined than the beam models used in the previous master theses on modular expansion joints. As the width of the centre beam top flange is divided in two plate elements there are three nodes on a row. Each node has a certain influence area, see Figure 7.9, which makes it possible to model the load on a node in time more accurate. Based on insight gained during the numerical analysis the idea rose that due to this influence area a single node is loaded over a longer time period by the maximum load value and that the cosine-shape is a too adverse representation for the loading. In addition to the cosine-shaped functions time history functions with a trapezium shape have been developed.

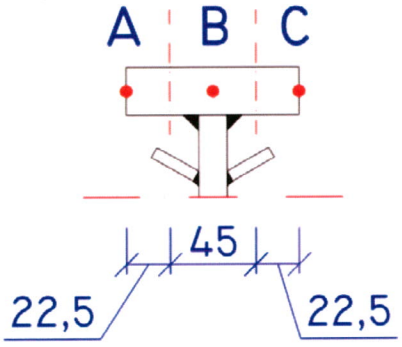

Figure 7.9 Influence area of the wheel for each node of the top flange.

For the dynamic nodal loads the arrival time and the time history changes when considering this influence area. The left end of the influence area now governs the arrival time to be applied to a node. If one looks at Figure 7.9 for example this means an arrival time for node C of
$(22,5+45) \cdot 10^{-3}$ m / 25 m/s = 0,0027 seconds in case of the first centre beam.
With regard to the time history functions two `function groups´ have been developed:

- The first group for influence areas A and C where the loading achieves its maximum value in $22,5 \cdot 10^{-3}$ / 25 = 0,9 ms. The total load duration is $322,5 \cdot 10^{-3}$ / 25 = 12,9 ms. The maximum value is ¼ of the maximum value for each load given in Table 7.2;
- The second group for influence area B where the loading achieves its maximum value in $45 \cdot 10^{-3}$ / 25 = 1,8 ms. The total load duration is $445 \cdot 10^{-3}$ / 25 = 17,9 ms. The maximum value is ½ of the maximum value for each load given in Table 7.2.

An impression of the trapezoidal time history function is shown in the figure below.

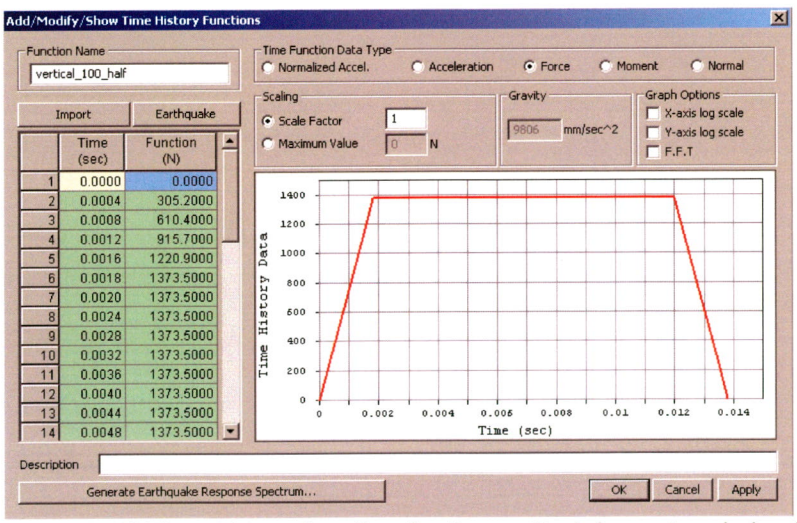

Figure 7.10 Time history function for the vertical dynamic axle load of 76,9 kN as applied to the middle part of the upper flange.

7.2.4. Modified reference model

All information presented the previous subparagraphs is devoted to the modelling of the WSG 320 joint in Bridge Heteren and the choices made during the process. This resulted in the so-called reference model. Since the moment that the modular expansion joints in Bridge Heteren were installed the design concept of WSG-type joint has slightly changed. Calculations made for the 'Regelprüfung nach TL/TP FÜ (Stand 03 / 05)' show for example shorter end fields (RW Sollinger Hütte GmbH, 2007).

In order to get an indication how the behaviour for the WSG 320 joint of Bridge Heteren would be influenced if it was designed according to the current design concept a couple of changes, which each were studied separate at first, are brought together in one new model. This finite element model is indicated as the modified reference model and contains the following modifications:

- The first support bar is shifted making the end field shorter;
- The dynamical stiffness in vertical direction is taken into account;
- The changed time history functions are applied.

The effects for each modification are also studied individually in the parameter study, as has been done for some other aspects. Obviously the results for this modified reference model will be compared with the reference model.

7.3. Analysis options

After entering the joint model and loads in the computer program choices had to be made concerning the analysis in order to obtain the desired output for post-processing step of the numerical analysis. First the options and values that have been chosen for the frequency analysis are described. Then the same is done for the time history analysis.

7.3.1. Eigenvalue analysis

Also known as a free vibration analysis, an eigenvalue analysis is used to analyse the dynamic characteristics of a structure. The output contains aspects such as vibration modes, natural periods of vibration and model participation factors. The latter are very convenient for determining which modes have the largest contribution to the free vibration. For all dynamic characteristics applies that they are governed by the mass and stiffness of the structure.

First some options with regard to the mass of the structure had to be selected. As the mass density of the structural members and the direction of gravity, with regard to self-weight, have been entered in previous steps this simplifies the work to be done. Options for conversion of structure self-weight into masses and conversion of these lumped masses to X-, Y- and Z-direction were selected.

Then options with regard to the control of the eigenvalue analysis were selected. The decision was made to perform the analysis using a Lanczos algorithm instead of subspace iteration, because the analysis is executed faster with this algorithm. Of course a free vibration analysis with subspace iteration would have given the same results.
For the number of frequencies to be calculated rather a high value has been chosen. During the various analyses fifty frequencies have been calculated. The decision has been made based on the output for the modal participation factors. When fifty frequencies are considered more than 90% of the total mass is included in an analysis. This will ensure that the critical modes that affect the results are included in the design[5]. It also became clear that mainly the higher frequencies give a large contribution to vertical motion. This will be discussed more thoroughly in paragraph 8.2, which deals with the results of the free vibration analysis.

[5] MIDAS/Civil 'Getting started'-manual, MIDAS Information Technology Co., Ltd. (2006).

7.3.2. Time history analysis

This analysis has to be performed in order to obtain the required output for calculation of dynamic factors and for a dynamic fatigue calculation. Of the time history data required for the analysis the time forcing functions and the dynamic nodal loads have already been discussed in paragraph 7.2.3. Now attention will be given to the time history load cases.

Only one single time history load case has been applied in the model and is used for every fatigue load combination. The options selected will be summarised in order of appearance in the program, and when necessary a brief description will be given.

The options and values chosen are:

- Analysis type: Linear time history analysis;
- Analysis method: Modal. For modal analyses MIDAS/Civil uses the modal superposition method, which is very effective and often used in linear dynamic analyses for large structures;
- Time history type: Transient. This means that during the analysis a time load function is carried out on the basis of only one load cycle;
- End time: a value of 0,1 s has been chosen for the duration of the analysis, because this is about three times longer than the loading time of a wheel with a length of 400 mm and provides enough time for the vibration to fade out;
- Time increment: a value of 0,5 ms has been entered. This value amounts about 1/10 of the highest modal period considered for the reference model;
- Damping: the modal damping method with a damping ratio of 0.095 for all modes is applied. This value of 9,5% has been chosen on the basis of the original design calculations and damping values found during recent over-rolling tests of modular expansion joints.

8. Numerical analysis

This chapter entails the post-processing phase in which the desired results obtained from the analysis output are presented. Before results were extracted from the output the reliability of the model had to be checked. How this was done is described in the first paragraph. In paragraph 8.2 the results of the frequency analysis are presented and compared with two analytical calculation methods.
Paragraph 8.3 deals with the dynamic factors that were derived from the results for the reference and modified reference model. Also is shown how certain aspects influence these factors and internal forces. Paragraph 8.4 shows the results of the dynamic fatigue analysis for the modified reference model. In the last paragraph an overview of this chapter is given.

8.1. Verification of the reference model

In order to be certain that reliable results are obtained with the finite element program the model needs verification. This was done with the use of results found during the analytical calculation.
The situation being compared is the fatigue load combination of a vertical axle force of 150 kN and a horizontal axle force of 20 kN. Here the dynamic factors $\Delta\varphi_{fat}$=1,3 and $\Delta\varphi_{fat,h}$=1,0 from Annex G (EOTA, 2006) are included in the loading as this was also the load case being used for the analytical calculation.
The output generated by the program together with the results of the analytical calculation is shown in Appendix VII and the results are presented in the table below. As can be seen the results found for the numerical analysis are about 1-10% lower. This could indicate that due to the more refined model better load distribution over the support bars occurs.

Table 8.1 Comparison results for the second support bar.

	Analytical calculation	Numerical analysis
Reaction forces for hinge support	47,30 kN	46,78 kN
Reaction forces for roller support	52,93 kN	49,37 kN
Bending moment at mid span	12,67 kNm	11,52 kNm

8.2. Natural frequency analysis

First two methods are described that are used for an analytical calculation of the first natural frequencies. Then the results that were found are presented. Concluding this paragraph the results are compared and conclusion are drawn.

8.2.1. Analytical calculation methods

From structural mechanics it is known that for a continuous bending girder the following applies:

$$f_v = \frac{\omega}{2\cdot\pi} = \frac{1}{2\cdot\pi}\cdot\sqrt{\frac{c}{m}} = \frac{1}{2\cdot\pi}\cdot\sqrt{\frac{K_{Bv}}{m}} = \frac{1}{2\cdot\pi}\cdot\sqrt{\frac{\frac{\pi^4\cdot E\cdot I_v}{L^4}}{m}} = \frac{\pi}{2\cdot L^2}\cdot\sqrt{\frac{E\cdot I_v}{m}} \quad [Hz]$$

As a centre beam can be regarded a continuous bending beam on multiple supports this formula has been used to determine the lowest vertical and horizontal frequencies.

NBD-00710
First the natural frequencies of the centre beams are considered. An important aspect to be taken into account is the length. The spacing between the support bars ranges from 1,85 m to 2,25 m. The length of the first middle field span, which is 2,00 meter, has been used in the calculation as it was considered the most favourable choice for the length L.

The vertical frequency for a centre beam has been calculated as follows:

$f_v = \pi /(2 * L^2) * \sqrt{(E * I_v / M)}$

with L = 2,00 m, E = 2,10 $\cdot 10^{11}$ N/m^2, I_v = 30,809 $\cdot 10^{-6}$ m^4 and M = 57,34 kg/m.

The frequency then is $f_v = \pi /(2 * 2^2) * \sqrt{(2,10 \cdot 10^{11} * 30,809 \cdot 10^{-6} / 57,34)} = 131,9$ Hz.

The horizontal frequency for a centre beam has been calculated as follows:

$f_h = \pi /(2 * L^2) * \sqrt{(E * I_h / M)}$

with L = 2,00 m, E = 2,10 $\cdot 10^{11}$ N/m^2, I_h = 3,212 $\cdot 10^{-6}$ m^4 and M = 57,34 kg/m.

The frequency then is $f_h = \pi /(2 * 2^2) * \sqrt{(2,10 \cdot 10^{11} * 3,212 \cdot 10^{-6} / 57,34)} = 42,6$ Hz.

Contrary to a centre beam, a support bar cannot be regarded as a continuous girder and therefore the situation shown on the left in Figure 8.1 has to be considered when determining the bending stiffness. Then the vertical frequency for the support bar was calculated as follows:

$f_v = 1/(2\pi) * \sqrt{(K_{bar} / M)}$

with $K_{bar} = 48 * EI / L^3 = 48 * 2,10 \cdot 10^{11} * 11,4 \cdot 10^{-6} / (0,677)^3 = 370,34 \cdot 10^6$ N/m and

$M = M_{bar} / 2 + (2 \text{ m} * 57,34 \text{ kg/m}) * 3 =$

$= (0,677 \text{ m} * 41,8 \text{ kg/m}) / 2 + (2 \text{ m} * 57,34 \text{ kg/m}) * 3 = 358,2$ kg.

The frequency then is $f_v = 1/(2\pi) * \sqrt{(K_{bar} / M)} = 1/(2\pi) * \sqrt{(370,34 \cdot 10^6 / 358,2)} = 161,8$ Hz.

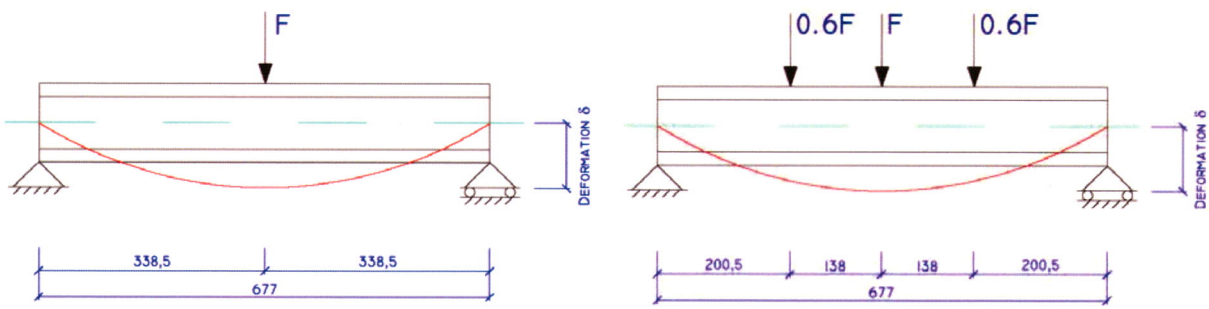

Figure 8.1 Left: Beam stiffness according to NBD-00710; Right: Alternative method.

Alternative method

For the calculation of the natural frequency for the support bar also another method has been applied in addition to the method according to NBD-00710. This method is based on the approach normally used by Sollinger Hütte. For this method the situation as depicted on the right in Figure 8.1 applies. With the use of a simplistic calculation program a vertical displacement of 5,24 $\cdot 10^{-3}$ m has been found after applying a unity load of 1000 kN.

With these values and the formula presented earlier, the following calculation was made:

$f_v = 1/(2\pi) * \sqrt{(K_G / M)}$

with $K_G = (2,2 * F) / \delta = 2,2 * 1 \cdot 10^6$ N / 5,24 $\cdot 10^{-3}$ m = 4,189 $\cdot 10^8$ N/m and

$M = M_{centre\ beam} + 0,6 * 2 * M_{centre\ beam} + M_{bar} / 2 =$

$= (2 \text{ m} * 57,34 \text{ kg/m}) + 0,6 * 2 * (2 \text{ m} * 57,34 \text{ kg/m}) + (0,677 \text{ m} * 41,8 \text{ kg/m}) / 2 = 266,5$ kg.

Then it follows that $f_v = 1/(2\pi) * \sqrt{(K_G / M)} = 1/(2\pi) * \sqrt{(4,189 \cdot 10^8 / 266,5)} = 199,75$ Hz.

8.2.2. Frequency results

Before the output of the numerical eigenvalue analysis is presented and discussed, the results found for the analytical calculation are summarised in the table below.

Table 8.2 Analytically calculated frequencies.

Member	Direction	NBD-00710	Alternative method
Centre beam	Vertical	131,9 Hz	-
	Horizontal	42,6 Hz	-
Support bar	Vertical	161,8 Hz	199,75 Hz

In paragraph 7.3.1 it has already been mentioned that during various analyses it was discovered that many eigenfrequencies have to be considered for the modal analysis. This will become clear when one looks at the output presented in Appendix VIII. The first part of this appendix shows the results for the reference model and the second part shows the results for the modified reference model. The most relevant results are also summarised in Table 8.3. In this table all modes are given that have a modal mass participation factor of at least 4%. When taking a look at these modal participation factors, it was noticed that the higher modes largely govern the vertical motion. Appendix IX shows the mode shapes belonging to the ten frequencies of the modified reference model that govern the three-dimensional movement of the expansion joint.

Table 8.3 Natural frequencies and modal masses participation factors.
Left: Reference model; Right: Modified reference model.

Mode Number	Frequency [Hz]	TRAN-X Mass [%]	TRAN-Y Mass [%]	TRAN-Z Mass [%]
1	22.57	5.09	0	0
3	23.02	4.55	0	0
7	45.68	25.26	0	0
8	51.84	24.31	0	0
11	56.24	19.28	0	0
17	93.94	0	12.51	0.43
19	107.59	0	79.29	1.91
34	132.82	0	0.88	16.25
37	139.63	0	0	16.66
39	144.27	0	0.09	28.73
47	152.14	0	0	13.33

Mode Number	Frequency [Hz]	TRAN-X Mass [%]	TRAN-Y Mass [%]	TRAN-Z Mass [%]
1	22.57	5.31	0	0
6	24.57	7.84	0	0
8	51.92	44.20	0	0
9	56.00	11.64	0	0
11	56.48	10.03	0	0
15	76.07	0	1.67	4.22
21	107.18	0	94.08	0
44	149.66	0	0.02	36.48
46	154.33	0	0.11	24.80
49	160.32	0	0	23.23

8.2.3. Reflection on the results

Unfortunaly the frequencies calculated for the centre beam and the support bar cannot be compared with the frequencies presented in Table 8.3 as these concern the complete system. Luckily there are other means available to make a comparison.
With the finite element program the eigenvector for a specific node can be normalized by displacement. In Appendix paragraph VIII.2 this is shown for the node at mid-span of the second support bar. The results indicate that the vertical translation is governed by mode number 44, which has a frequency of 149,66 Hz. This lies close to the value of 161,8 Hz calculated with the Bouwdienst standard NBD-00710.

Table 8.4 Comparison of natural frequencies.

	Vertical	Horizontal
Original design calculations[6]	94,9 Hz	38,6 Hz
Regelprüfung[7]	125,1 Hz	54,9 Hz
Numerical analysis – reference model	93,9 Hz	22,6 Hz
Numerical analysis – modified model	76,1 Hz	22,6 Hz

Literature from Sollinger Hütte provided the other information for making a comparison with the output obtained for the numerical analyses. Values were found in the original design calculations and the calculations made for the 'Regelprüfung nach TL/TP FÜ (Stand 03 / 05)'. These values are given in Table 8.4. It should be noted the second document does not concern calculations for Bridge Heteren, but WSG-type joints with shorter end fields. The frequencies for the two models studied during the numerical analysis are the first natural frequencies. If the vertical and horizontal frequencies belonging to the first modes with a high modal mass participation factor (> 10%) are considered, see Table 8.3, it can be seen that these frequencies are higher than those from the literature.
An important conclusion that can be drawn from the frequency analysis is that although lower natural frequencies are found, the modes with higher frequencies govern the system behaviour.

[6] Sollinger Hütte GmbH (1999).
[7] RW Sollinger Hütte GmbH (2007).

8.3. Dynamic factors

In the past different methods have been used for determining the dynamic amplification factors of a structural system. Ancich et al. (2006) for example determine dynamic factors from the maximum displacements. Here an approach has been applied where the relevant dynamic factors are calculated from the internal bending moments. It is believed that this approach is more favourable as the internal forces apply to the whole cross-section of a structural member, whereas displacements concern only one point of a cross-section. Secondly, the internal moments are also the required input for a fatigue analysis contrary to displacements.
Three different dynamic amplification factors investigated are the first dynamic amplitude, the upswing ratio and the total dynamic interval. The following definitions are handled for calculation of these dynamic factors:

- The first dynamic amplitude is found by dividing the first maximum value for the dynamic moment by the static value;
- The upswing ratio can be calculated by taking the absolute value of the first dynamic amplitude plus the first upswing moment, and then divided by the first dynamic amplitude;
- The total dynamic interval is the product of the first dynamic amplitude and the upswing ratio.

These three definitions are also presented in the same order of appearance in the formulas below.

$$\varphi_1 = \mathrm{M}_{\mathrm{dynamic}}/\mathrm{M}_{\mathrm{static}}$$

$$\varphi_2 = \left(\mathrm{M}_{\mathrm{dynamic}} + \mathrm{M}_{\mathrm{upswing}}\right)/\mathrm{M}_{\mathrm{dynamic}} = 1 + \left(\mathrm{M}_{\mathrm{upswing}}/\mathrm{M}_{\mathrm{dynamic}}\right)$$

$$\mathrm{Dynamic\,interval} = \varphi_1 \times \varphi_2$$

With the analysis program graphs can be generated showing the value of the bending moment as a function of time. This can very easily be done for the support bars as they are beam elements and by doing so all required dynamic moments are known.
For the centre beams these time-moment-graphs cannot be generated and a more complex approach had to be followed in order to obtain the internal moments. Time-displacement-graphs have been made for the node at half the height of the profile, i.e. node 2936 and 2942 as shown in Figure 8.2. From these graphs the points in time have been determined at which dynamic amplification reaches the maximum values. Then the corresponding plate stresses were obtained from the time-history output, and thus providing the stress diagrams from which the vertical and horizontal bending moment could be derived. For the reference model calculation of the bending moments from the stress diagrams is shown in Appendix X.

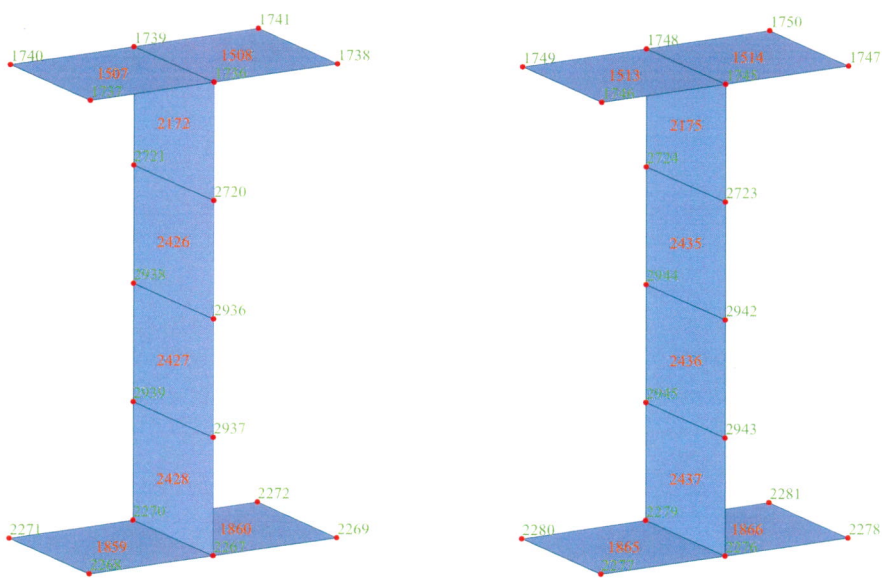

Figure 8.2 Cut-out with node and element numbers for the second centre beam at the mid-span of the end field. Left: The reference model; Right: The modified reference model.